

University of
Strathclyde
Glasgow

Department of Mechanical and Aerospace Engineering

**Design and Analysis of Wind Turbines for Favourable
Locations in Malawi**

Author: Chimwemwe Chisembe (202354373)

Supervisor: Dr Stephanie Ordonez Sanchez

A thesis submitted in partial fulfilment for the requirement of degree in
Master of Science in Renewable Energy Systems and the Environment

2024

Word Count: 13393

Copyright Declaration

This thesis is the result of the author's original research. It has been composed by the author and has not been previously submitted for examination which has led to the award of a degree.

The copyright of this thesis belongs to the author under the terms of the United Kingdom Copyright Acts as qualified by University of Strathclyde Regulation 3.50. Due acknowledgement must always be made of the use of any material contained in, or derived from, this thesis.

Signed:



Date: 12/08/2024

Abstract

Malawi is a country that has set high targets for itself in terms of development as elaborated in the Malawi vision 2063. Key to the development is sustainable energy supply. One of the sources is wind energy which is growing at a rapid rate worldwide. Research has been done in Malawi that has identified six suitable sites (in five districts) for wind turbine installation. This study then used this knowledge to understand how three turbines: 1.25 MW, 2.5 MW and 3.5 MW downscaled from the NREL 5 MW reference turbine would perform in these sites at different hub heights of 50 m, 80 m, and 100 m.

QBlade software which uses the Blade Element Momentum Theory (BEMT) was used for analysis. It was found that, out of the three turbines, two turbines had capacity factors which were not significantly different from the global onshore wind turbine capacity factor range of 21-52 percent: 2.5 and 3.5 MW turbines with capacity factors of 21 and 19.7 percent respectively. These were achieved at a hub height of 100 m in Mzimba district indicating that Mzimba is a very good location for further wind turbine technology exploration. The highest annual energy produced (AEP) was also in Mzimba at 100 m with the 3.5 MW turbine producing an AEP of 6.68 GWh. This annual energy produced would serve 719 urban buildings and 1845 rural buildings which is well short of the findings by Chisale & Lee (2024) [1]. The discrepancies call for further analyses and that they should be focused on turbines with low specific power due to the low wind speeds in Malawi.

Acknowledgements

I would like to express my deepest gratitude to Dr. Stephanie Ordonez Sanchez for her support and her expert insights which helped me navigate throughout the course of project. Not only that, I have also learnt a lot from her in terms of time management and organisational skills. She was always present and on time for meetings although she is a busy individual. I will take these skills with me as I continue on my professional journey. I would also like to thank Dr. Daniel Costola for his constructive inputs during the interim presentation which was instrumental in shaping the final report.

Table of Contents

Copyright Declaration.....	ii
Abstract.....	iii
Acknowledgements.....	iv
Table of Contents.....	v
List of Figures.....	vii
List of Tables.....	viii
Nomenclature.....	ix
Abbreviations.....	1
1.0 Introduction.....	2
1.1 Background.....	2
1.2 Introduction to the Problem.....	2
1.2.1 Overall Aim.....	3
1.2.2 Specific Objectives.....	3
1.2.3 Thesis Structure.....	3
2.0 Literature Review.....	4
2.1 Malawi’s Energy Situation.....	4
2.1.1 Hydropower.....	4
2.1.2 Biomass.....	4
2.1.3 Solar PV.....	5
2.1.4 Diesel.....	5
2.1.5 Wind Energy.....	5
2.2 Wind Energy Potential in Malawi.....	6
2.3 Wind Turbine Technology.....	7
2.4 Design Considerations for Wind Turbine.....	11
2.4.1 Aerodynamic Theory.....	11
2.5 Blade Element Momentum Theory (BEMT).....	11
2.6 QBlade Software Review.....	15
2.7 The 5 MW NREL Reference Turbine.....	15
3.0 Methodology.....	18
3.1 Favourable Sites Considerations.....	18
3.2 Scaling Study.....	19
3.2.1 Rotor Diameter.....	20

3.2.2 Rotor Speed.....20

3.2.3 Chord Length21

3.2.4 Rotor Nacelle Assembly Mass.....21

3.3 QBlade.....21

3.3.1 Wind Speed Data22

3.4 Power Curve.....23

3.4.1 Annual Energy Production (AEP)24

3.4.2 Capacity Factor (C_f).....26

4.0 Results and Discussion28

4.1 Rotor Dimensions.....28

4.2 Rotational Speed28

4.3 Chord Length.....29

4.4 Rotor Nacelle Assembly.....30

4.5 Energy Production.....31

5.0 Conclusion and Further Work.....37

6.0 References.....39

List of Figures

Figure 1: Malawi’s Installed Electricity Capacity in 2022 [5]	4
Figure 2: Wind Power Capacity Worldwide [17]	6
Figure 3: Wind turbine components [26].....	8
Figure 4: Wind turbine configurations (a) VAWT, (b) HAWT [29], [30]	10
Figure 5: The Development Path and Growth of Wind Turbines [35]	11
Figure 6: Definition of forces, angles, and velocity for the propeller blade [42].	12
Figure 7: Idealized Flow Model for the (Froude-Rankine) Momentum Theory [42], [43].....	13
Figure 8: QBlade airfoil design module.....	22
Figure 9: Generic Power Curve of a Wind Turbine.....	24
Figure 10: Wind Speed-Frequency Weibull Distribution Curve [78]	25
Figure 11: Power Curves for C_f Explanation [80]	26
Figure 12: Power Curves of the Turbines	31
Figure 13a, b, c: Annual Energy Yield of the Turbines.....	32
Figure 14a, b, c: Capacity Factors of the Turbines	33
Figure 15: C_f Patterns for a Site in Mzimba	34
Figure 16: Power Curves of G114-2.5MW and V136-3.45 Turbines [1].....	35

List of Tables

Table 1: Wind Turbine Classifications [26].....	8
Table 2: 5 MW NREL Reference Turbine Specifications [52]	15
Table 3: Distributed Blade Aerodynamic Properties [52]	16
Table 4: Rotor Dimensions	28
Table 5: Rotational Speed Results	29
Table 6: Airfoil Chord Length	29
Table 7: Nacelle Assembly Mass.....	30

Nomenclature

<u>Symbol</u>	<u>Description</u>	<u>Units</u>
C_l	Coefficient of lift	-
C_d	Coefficient of drag	-
ρ	Density of Material	kg/m^3
φ	Helix Angle	$^\circ$
α_i	Angle of Attack	$^\circ$
ω	Angular Velocity	rad/s
α	Wind Shear Coefficient	-
A	Area	m^2
c	Chord Length	m
C_P	Coefficient of Power	-
D	Diameter	m
R, r	Radius	m
dD	Differential Drag	N
dL	Differential Lift	N
dQ	Differential Torque	Nm
dr	Annular Segment	m
dT	Differential Thrust	N
P	Available Power	W
m	mass	kg
V, U, v	velocity	m/s
dF _Q	Differential Force	N
P	Pressure	Pa
a	Axial Induction Factor	-
h	Hub Height	m
λ	Tip Speed Ratio	-
f_v	Frequency of Wind Speed	%

Abbreviations

CO ₂	Carbon Dioxide
ADGs	African Development Goals
GHG	Greenhouse Gas
NREL	National Renewable Energy Laboratory
MW	Megawatt
BEMT	Blade Element Momentum Theory
PV	Photovoltaic
IPP	Independent Power Producer
MET	Meteorological Office
AGL	Above Ground Level
ERA5	Fifth Generation of Atmospheric Reanalysis
MERRA-2	Modern-Era Retrospective analysis for Research and Applications, Version 2
WRF	Weather Research & Forecasting
GIS	Geographic Information System
AHP	fuzzy Analytic Hierarchy Process
kW	Kilowatt
GWh	Gigawatt-Hour
USTDA	US Trade and Development Agency
HAWT	Horizontal Axis Wind Turbines
VAWT	Vertical Axis Wind Turbines
CFD	Computational Fluid Dynamics
DMST	Double Multiple Stream Tube
LLT	Lifting Line Theory
rpm	Revolutions per Minute
TSR	Tip Speed Ratio
WindPACT	Wind Partnership for Advanced Component Technologies
RECOFF	Recommendations for Design of Offshore Wind Turbines
DOWEC	Dutch Offshore Wind Energy Converter
NACA	National Advisory Committee for Aeronautics
DU	Delft University
PBL	Planetary Boundary Layer
km	Kilometre
RNA	Rotor Nacelle Assembly
at	Axial Turbine
AEP	Annual Energy Production
IEC	International Electrotechnical Commission
GE	General Electric

1.0 Introduction

1.1 Background

Demand for energy is growing in Africa and globally with advancements in technology and improvement of lifestyle. However, despite the ample resources at its disposal, Africa's modern energy use per capita is still very low with just 6 percent of global energy use. As a result, it contributes to only less than 3 percent of the world's carbon dioxide (CO₂) emissions [2]. This statistic implies that there is a lot of untapped energy in Africa that needs exploration so that the number of 600 million people without access to electricity in the continent can be reduced sooner rather than later.

In line with the African Development Goals (ADGs), efforts are being made in terms of finances so much so that it is expected that by 2030, energy spending in Africa will be more than double with more than two thirds of the energy being clean energy. Therefore, many countries in Africa including Malawi have embarked on various research systematically tailored to the achievement of the ADGs including increase in energy access and reducing greenhouse gas (GHG) emissions [2], [3], [4].

Malawi, a landlocked country in south-eastern Africa, relies heavily on hydroelectric power to meet its energy demands. Hydropower accounts for over 90 percent of the country's grid electricity generation [5], primarily sourced from the Shire river. This heavy dependence on a single energy source has left Malawi vulnerable to significant energy supply challenges. Periodic droughts and changing climatic conditions have led to inconsistent water levels, directly impacting the country's ability to generate sufficient electricity [6]. As a result, Malawi experiences frequent load shedding, adversely affecting its socio-economic development [7].

1.2 Introduction to the Problem

The persistent issue of load shedding in Malawi underlines the urgent need for a more diversified and resilient energy mix. While hydropower remains a vital component of the country's energy strategy [8], exploring alternative renewable energy sources is of vital importance to ensure a stable and sustainable electricity supply going forward.

Among the various renewable energy options, wind energy presents a promising yet underexplored opportunity in Malawi. The little research that has been done on wind energy in Malawi has focused more on the demand without delving deep into how the turbines would really perform. There has been minimal research on identifying the

most suitable wind turbine designs for the country's specific conditions. This gap in knowledge hinders the effective harnessing of the wind energy and limits the overall energy diversification efforts which the country endeavours for. It is therefore high time this area is studied and researched on to reduce Malawi's dependence on hydropower and achieve a more sustainable power supply.

1.2.1 Overall Aim

This research's aim is to design and evaluate the performance of three wind turbines in QBlade scaled down from the standard National Renewable Energy Laboratory (NREL) 5 MW turbine at different hub heights in favourable locations for wind energy exploration in Malawi to then see which turbine is the most effective turbine design for harnessing wind power in Malawi.

1.2.2 Specific Objectives

The specific objectives of this report are:

- To conduct a comprehensive assessment of wind energy potential across Malawi, identifying suitable sites based on wind patterns, terrain, and available resources for wind turbine installations.
- To scale down the NREL 5 MW turbine to 3.5, 2.5, and 1.25 MW turbines for analysis in QBlade.
- To incorporate site-specific data into QBlade to get power curves for AEP analysis.

1.2.3 Thesis Structure

The thesis begins with a review of literature that includes a summary on Malawi's energy profile, and also wind resource assessments as regards to the country. This is followed by a review on wind turbine technology and the blade element momentum theory (BEMT) which is the theory used by QBlade software to analyse the turbines.

Then the report delves into the methodology part where site considerations parameters, scaling and the QBlade inputs are explained.

Finally, the study discusses the findings which is then followed by the conclusion and recommendations for further work as far as wind energy projects in Malawi are concerned.

2.0 Literature Review

2.1 Malawi's Energy Situation

2.1.1 Hydropower

Currently, hydropower constitutes about 70 percent of Malawi's energy mix [5] and over 85 percent is renewable energy (Figure 1).

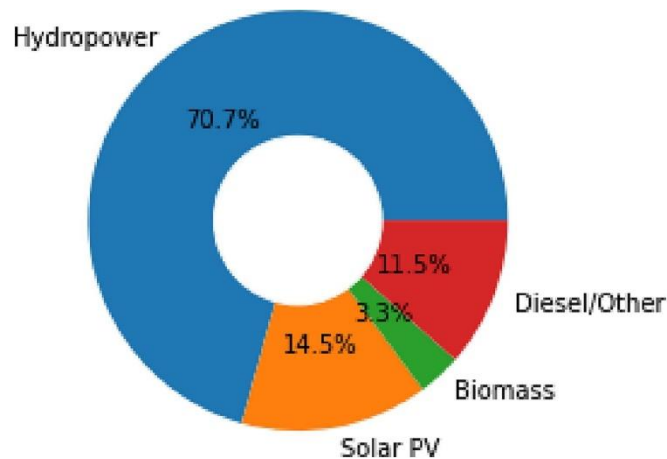


Figure 1: Malawi's Installed Electricity Capacity in 2022 [5]

Looking at these figures, one would conclude that Malawi is on the right path in as far as sustainability is concerned however while that may be true to some extent, with an electrification rate of 18 percent [5] there is need for more reliable power supply if Malawi is to make significant strides towards economic development. It is worth pointing out that hydro power is responsible for 98 percent of electrical grid electricity [9] which renders the country prone to consistent power outages when there are problems at the generation plants. This necessitates the need for the diversification of the energy mix by exploring other sources of energy, in particular renewable energy sources, because the world is going towards renewable to try to mitigate the effects of climate change.

2.1.2 Biomass

Biomass energy in Malawi is derived from organic materials such as agricultural residues and wood. It plays a crucial role in the country's energy mix by providing a renewable source of power – mainly for cooking and heating – particularly in rural areas. Wood and charcoal, which are mostly sourced unsustainably as well [10], are in fact used by over 86 percent of Malawians [11]. This increases the rates of

deforestation and forest degradation in Malawi which contribute to the country's vulnerability to climate shocks [6].

However, when it comes to electricity generation, Malawi only has one biomass power plant with a maximum capacity of 10 MW [12]. The overall electricity installed has since increased in Malawi to 441.6 MW [13] which has resulted to the percentage of the biomass plant to drop to 2.3 percent from 3.3 percent in 2021 (Fig. 1).

2.1.3 Solar PV

Solar photovoltaic (PV) systems convert sunlight directly into electricity. Malawi has seen an increase in solar PV installations, contributing to the diversification of its energy mix. Currently there is 102.3 MW worth of electricity from solar plants with more projects proposed by independent power producers (IPPs) in the pipeline [11].

Solar energy is widely available and can be deployed at various scales, from small residential systems to large utility-scale plants. However, solar power generation is intermittent, requiring storage solutions e.g., batteries or complementary systems to ensure a consistent power supply which increase the costs associated with the technology. Despite this, the global cost of solar PV technology is decreasing [14] which makes it an attractive option for expanding renewable energy capacity in Malawi.

2.1.4 Diesel

Malawi has 7 stations with diesel generators installed used in an “emergency or standby power supply”. They are also used to meet peak demand [15].

While diesel is a reliable source of electricity, it is also the most polluting and expensive in terms of fuel costs and maintenance. This was evident in 2022 when the government of Malawi spent one hundred and seventeen billion Malawi kwacha (K117 billion) which prompted the nation to reflect on how best to use its already slim budget [16]. It is therefore best to transition away from diesel to cleaner and more sustainable energy sources. This will not only reduce GHGs, but also save on the stretched national budget.

2.1.5 Wind Energy

Although wind energy is not yet part of Malawi's energy mix (Fig. 1), it presents a promising opportunity for diversification. Globally it is ever growing with 2023 being

a record year (Fig. 2) [17]. This growth means that prices will continue to drop and drop making the technology more economically viable.



Figure 2: Wind Power Capacity Worldwide [17]

Wind turbines convert kinetic energy from wind into electricity, offering a renewable and low-carbon energy source [18]. Wind power can be variable and site-specific, necessitating careful site selection and grid integration strategies. Developing wind energy infrastructure could complement Malawi's existing hydropower and the expanding solar PV systems, enhancing the nation's overall energy resilience and sustainability.

2.2 Wind Energy Potential in Malawi

Previous studies on wind energy in Malawi have identified several regions with promising wind resources. Wind speed data has been recorded by the Malawi department of climate change and meteorological services (MET) at 2 m and 10 m above ground level (AGL) over the years with its fair share of problems such as inconsistencies and data missing as found from one of the initial feasibility studies on wind energy resource assessment in Malawi by the University of Strathclyde in 2012 [19].

Based on the same 'unreliable' data from MET, Malunga (2019) found that turbines with a cumulative rating of 30 MW could be installed at certain 'favourable sites' (high wind speed areas). The number of turbines that could be installed depended on the land available at the favourable sites. For instance, he states that four turbines of 2 MW rating could be erected at the favourable sites in Lilongwe and Mzimba, five turbines

in Blantyre, and two turbines in Mzuzu [20]. Installing turbines based on this data would not be very practical because of the inconsistencies in the recorded data and some missing values, plus wind speeds at AGLs close to the ground are heavily influenced by load sheltering and surface roughness effects [1].

In view of this, Chisale & Lee (2024) [1] did a study where they analysed the wind speeds at 80 m and 100 m hub heights. They utilised the open-source Weather Research & Forecasting (WRF) model which uses the ERA5 reanalysis data and validated it against the MERRA-2 dataset – which were in agreement – to get high resolution wind speed data with accuracy levels of up to 98 percent achieved in Brazil [21], and similar percentages in Chile [22]. Despite the model being too complex since it has to be integrated with the geographic information system (GIS) and fuzzy analytic hierarchy process (AHP) [1], it gives more precise and reliable wind farm location data. The model gave six favourable sites in Dedza, Kasungu, Ntchisi, Mzimba (2 sites), and Chitipa with annual average wind speeds of between 6.99-8.72 m/s and a corresponding power density range of 170-331.37 W/m² at 80 m, and wind speeds of between 7.04-8.76 m/s and power density range of 174.30-336.65 m/s at 100 m.

More research has been done on wind in Malawi but with little success. For instance, research was done by Zalengera (2015) on a micro grid consisting of wind, solar and generator for Likoma Island. For wind energy, a 10 kW wind turbine with 3 m/s cut-in speed was chosen and analysed from numbers 0 to 175 at varying heights: 10 m, 25 m, 40 m and 50 m. 40 m was concluded to be the optimum with average speeds from 3.58 m/s to 5.14 m/s [23]. However, currently electricity on the island is only provided by solar PVs and generators [24].

The government of Malawi has also conducted a feasibility study where it was found that twenty-nine Vestas V126-3.6MW turbines could be installed at a hub height of 117 meters to give an annual energy production of 510 GWh [25]. A report on this study is not available but the capacity factor is about 56 percent which is a pretty high number considering the wind speed data in the district and the results found in this research, further underlining the need for more detailed assessments.

2.3 Wind Turbine Technology

There are several components that make up a wind turbine including blades, rotor, nacelle, gearbox, generator and the tower (Fig. 3).

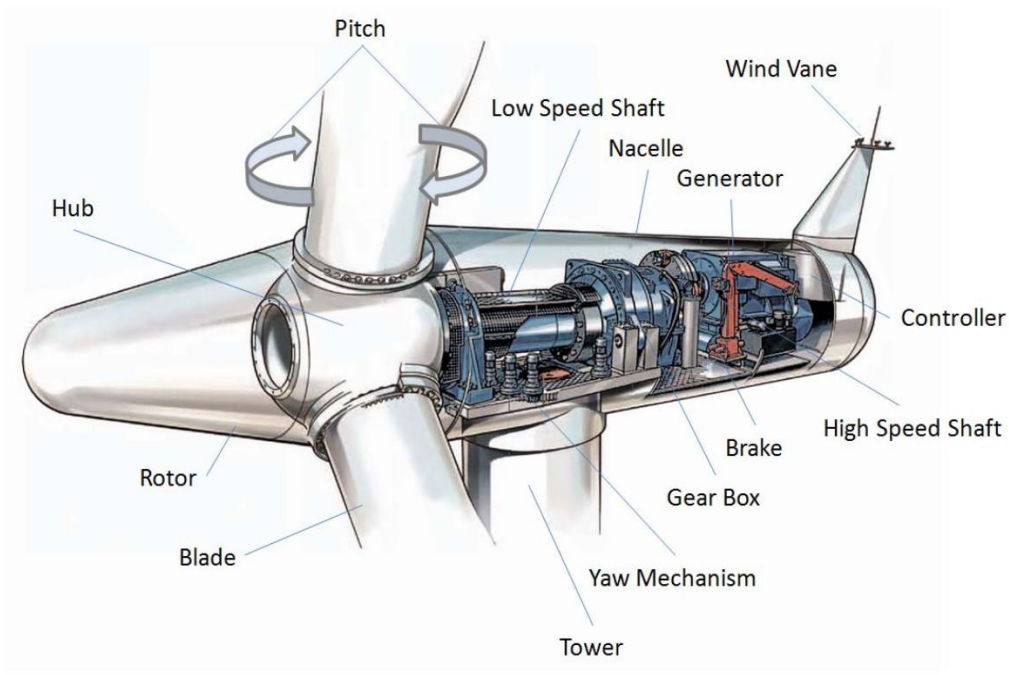


Figure 3: Wind turbine components [26]

These components make it possible for the turbine to convert kinetic energy to electricity. For instance, the blades capture wind energy and then convert it into rotational motion which is then transferred through the rotor and gearbox to the generator producing electricity. The nacelle houses all of these components and is mounted on top of the tower which is the pillar for the turbine [26].

Turbines are classified into three types based on how large they are and production capacity: utility scale, industrial/commercial scale, and residential scale [26] (Tab. 1).

Table 1: Wind Turbine Classifications [26]

Classification	Energy Production (per Turbine)	Applications
Utility-Scale (Large Turbines)	1 MW – 10 MW	<ul style="list-style-type: none"> Typically installed in “wind energy” projects. Generate bulk energy for sale in power markets. Can be installed in small quantities on distribution lines (distributed generation).
Industrial-Scale (Medium-Sized Turbines)	50 kW – 250 kW	<ul style="list-style-type: none"> Typically used in light commercial/industrial and village power applications. Intended for remote grid production, often in conjunction with diesel generation or load side generation (on the customer’s side of the meter) to reduce consumption of higher cost grid power and reduce peak loads.

		<ul style="list-style-type: none"> • Direct sale of energy to local utility may be allowed, depending on state law or utility regulations.
Residential-Scale (Small-Scale or Micro Turbines)	400 watts – 50 kW	<ul style="list-style-type: none"> • Used by small businesses, farms, and individual homes. • Intended for remote power, battery charging, or net metering (utilities have to give credits to customers if they generate more power than they get from the grid). • Small turbines can be used with solar photovoltaics, batteries, and inverters to provide constant power at remote locations where installation of a distribution line is more expensive or not feasible

Utility scale turbines are large turbines of not less than 1 MW rated power output which are usually installed with the aim of feeding the grid electricity for bulk electric power sales. Industrial scale are medium sized turbines that are usually between 50 kW to 250 kW of rated output. They can be used to feed the grid and also, like the residential small-scale turbines, for remote power where grid connection is not possible or too expensive. It therefore depends on the need and the finances available on which turbine to install. For this research, utility scale turbines were designed for analysis because Malawi plans to develop a 150 MW wind farm [27] – currently in the dormant state – and a 50 MW wind farm which has recently been supported, in form of a grant, by the US Trade and Development Agency (USTDA) [28]. Therefore, research on how utility scale turbines would perform in the country can aid the developers of these intended wind farms.

There are two main types of wind turbines: Horizontal Axis Wind Turbines (HAWTs) and Vertical Axis Wind Turbines (VAWTs) (Fig. 4).

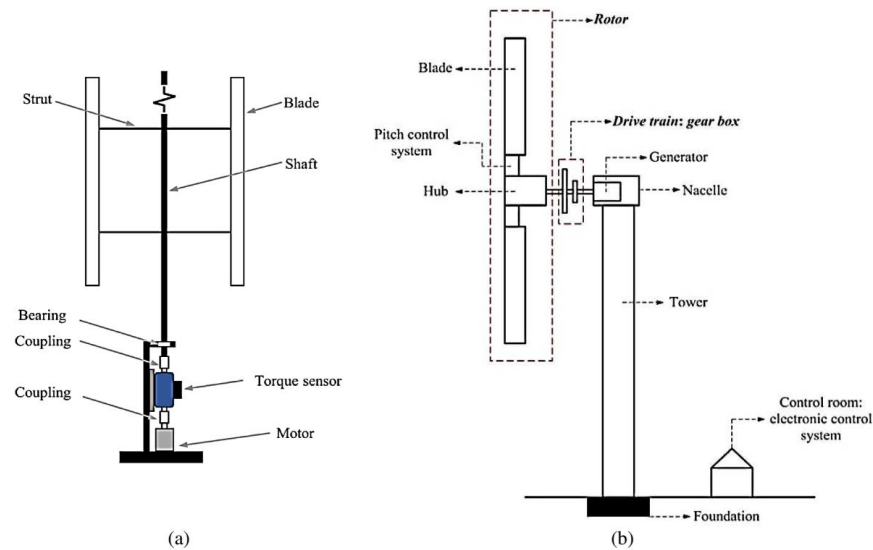


Figure 4: Wind turbine configurations (a) VAWT, (b) HAWT [29], [30]

HAWTs are the most common and efficient type, featuring a rotor with blades that rotate around a horizontal axis. VAWTs have blades that rotate around a vertical axis and can capture wind from any direction. HAWTs however usually operate in the upwind design where the blades are in front of the nacelle. The design must also have a yaw mechanism so that the rotor is always facing in the direction of the wind. Downwind designs are also possible but the mostly used in industry are the upward machines [26], [30].

Recent research in wind turbine design has focused on increasing efficiency, reducing costs, and enhancing reliability. These advancements include larger rotor diameters and taller towers (Fig. 5), and improved blade aerodynamics [31].

Furthermore, the use of advanced materials, such as carbon fibre composites, has led to lighter – 25 percent blade mass reduction – and stronger blades. Additionally, “the new textile-based carbon fibre material used for spar caps cost 40 percent less than commercial carbon fibre potentially enabling the broader adoption of carbon fibre materials in wind turbine blade design with the potential to reduce system costs” [32], [33]. Also, innovations in control systems and predictive maintenance technologies are improving the performance and longevity of wind turbines [34]. That is why turbines continue to increase in size and height as the years pass.

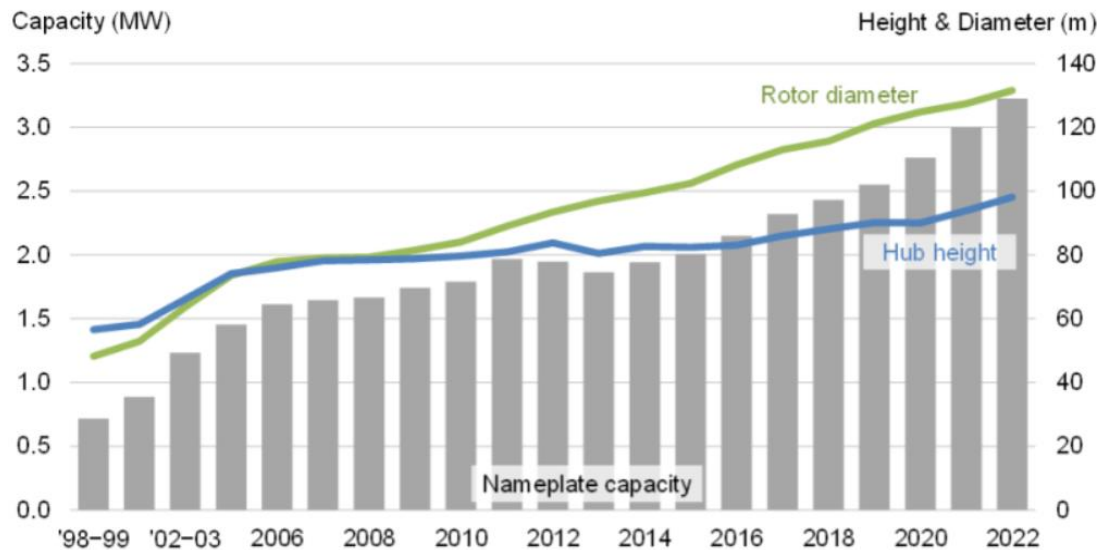


Figure 5: The Development Path and Growth of Wind Turbines [35]

Figure 5 shows how much the wind turbine sizes have increased with time. Research shows that the larger the turbine size, the larger the capacity because the swept area is large as well.

2.4 Design Considerations for Wind Turbine

Several factors influence wind turbine design, including wind speed, turbulence, environmental conditions, and site-specific characteristics such as closeness to road network, grid connection etc. These then influence the choice of rotor diameter, hub height, and blade materials which directly impact energy capture and overall efficiency.

2.4.1 Aerodynamic Theory

The aerodynamic design of wind turbine blades is crucial for maximizing energy capture because it regulates the movement of the wind around the blades [36]. Blades are designed to have an optimal airfoil shape that generates lift and minimizes drag. Computational tools, such as Blade Element Momentum Theory (BEMT) and Computational Fluid Dynamics (CFD), are used to simulate and optimize blade performance under various wind conditions [37].

2.5 Blade Element Momentum Theory (BEMT)

The blade element momentum theory (BEMT) is heavily applied in the design and analysis of wind turbines. It combines the principles of two theories; blade element

theory and momentum theory, to predict the aerodynamic performance of turbine blades.

i. Blade element theory

“Blade element theory assumes that blades can be divided into small elements that act independently of surrounding elements and operate aerodynamically as two-dimensional airfoils whose aerodynamic forces can be calculated based on the local flow conditions” [38]. The total forces and moments exerted on the blade can then be calculated using coefficients of lifts and drag, C_l and C_d , along with the respective angle of attack summed up for each element along the entire blade [38], [39], [40], [41]. The differential forms of lift and drag forces of the element are shown in Equations 1 and 2:

$$dL = 0.5\rho V_E^2 \cdot c \cdot C_l \cdot dr \quad \text{Equation 1}$$

$$dD = 0.5\rho V_E^2 \cdot c \cdot C_d \cdot dr \quad \text{Equation 2}$$

Where ρ is the density of the wind (air), V_E is the velocity of the airflow approaching the element as shown in Figure 6, c is the chord length of the element, and the coefficients of lift and drag of the element airfoil are given as C_l and C_d [41], [42].

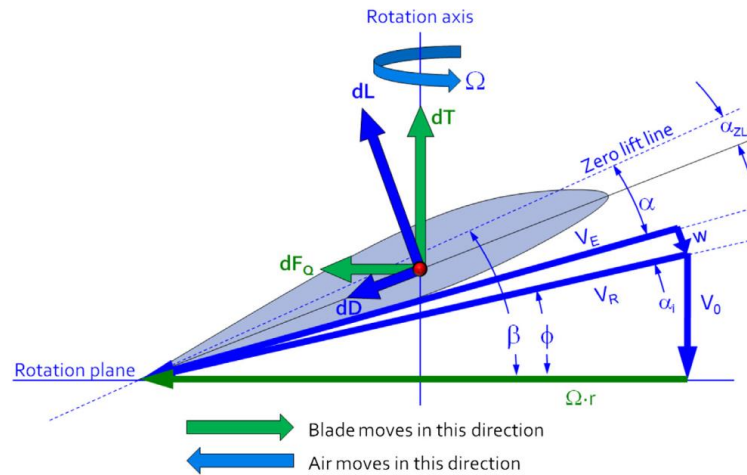


Figure 6: Definition of forces, angles, and velocity for the propeller blade [42].

From equations 1 and 2, differential thrust and torque can then be calculated as:

Differential thrust:

$$dT = dL \cos(\phi + \alpha_i) - dD \sin(\phi + \alpha_i) \quad \text{Equation 3}$$

Differential torque:

$$dQ = r \cdot dF_Q = r[dL \sin(\phi + \alpha_i) - dD \cos(\phi + \alpha_i)] \quad \text{Equation 4}$$

And therefore, differential power as:

$$dP = \Omega r \cdot dF_Q = \Omega r[dL \sin(\phi + \alpha_i) - dD \cos(\phi + \alpha_i)] \quad \text{Equation 5}$$

where F_Q is force.

ii. Momentum theory

The momentum theory also known as the actuator disk theory “assumes that the loss of pressure or momentum in the rotor plane is caused by the work done by the airflow passing through the rotor plane on the blade elements” [38].

The theory can be used to estimate propeller thrust by allowing the airspeed inside the propeller stream tube to be estimated (the so-called propeller-induced velocity).

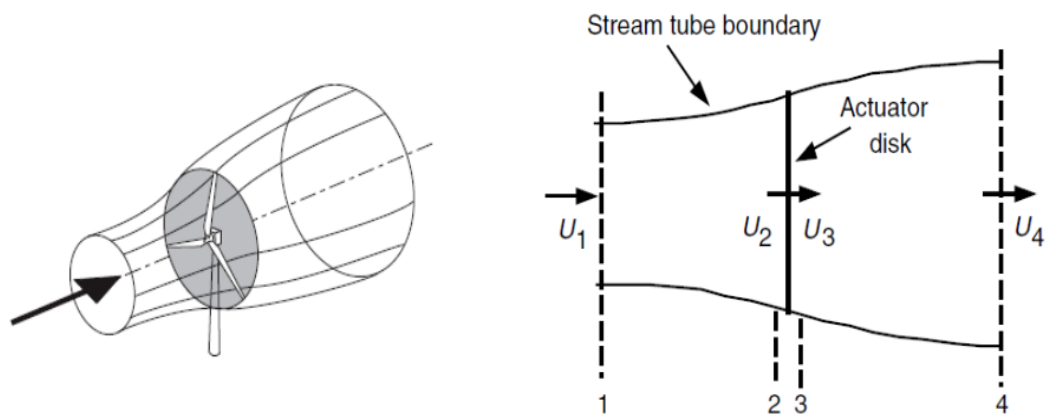


Figure 7: Idealized Flow Model for the (Froude-Rankine) Momentum Theory [42], [43]

The results however are generally optimistic because the theory comes with seven assumptions including: frictionless flow, ideal incompressible fluid at steady flow, pressure entering and leaving are equal and zero wake on the system [42].

These assumptions allow the Bernoulli’s principle to apply where P_2 and P_3 can then be calculated using the known unperturbed pressure conditions on plane 1 and plane 4 from Figure 7 respectively [42]. As the wind flows through the disk, pressure decreases due to the loss in energy of the wind stream – because the disk exerts a retarding force on the stream and extracts energy from it – and then approaches the initial pressure as the wind moves close to the end of the control volume at plane 4 [38], [41]. Therefore, the pressure difference between P_2 and P_3 can be calculated using:

$$P_2 - P_3 = \frac{1}{2} \rho (U_1^2 - U_4^2) \quad \text{Equation 6}$$

After several derivations, it can be deduced that the power P that the rotor extracts is:

$$P = \frac{1}{2} \rho A U^3 \quad \text{Equation 7}$$

Where ρ is the air density, A is the circular area swept by the rotor blades and U is the wind speed.

Not all the energy from the wind is extracted. There is a theoretic limit that the rotor can harness energy from the wind stream. This is called the Betz limit sometimes referred to as the power coefficient C_p .

After further derivations from the momentum theory above, C_p is found by:

$$C_p = \frac{P_{out}}{\frac{1}{2} \rho A U^3} = 4a(1-a)^2 \quad \text{Equation 8}$$

which reaches a maximum $a = 1/3$ after equating the first derivative dC_p/da to zero, leading to:

$$C_{pmax} = \frac{P_{max}}{\frac{1}{2} \rho A U^3} = \frac{16}{27} = 0.593 \quad \text{Equation 9}$$

Considering this limit, Eqn. 7 can then be written as:

$$P = C_p \cdot \frac{1}{2} \rho A U^3 \quad \text{Equation 10}$$

Knowing that the area swept by the rotor is that of a circle, Eqn. 10 can be written as:

$$P = C_p \cdot \frac{1}{2} \rho U^3 \pi \cdot r^2 \quad \text{Equation 11}$$

Where r is the radius of the rotor, ρ is the air density, U is the wind speed, C_p is power coefficient.

BEMT therefore, divides the blade into small elements and calculates the forces and moments acting on each element to determine the overall performance [37], [44].

While it is fairly accurate, it was not the case in previous years because BEMT is not advanced enough to handle complex three-dimensional flows due to the blade system's rotation [37]. However, research has been done by several scientists including Mikkelsen and Madsen to improve this theory.

Mikkelsen carried out a study to verify the assumptions inherent BEMT and found that the maximum resulting error was 3 percent [40] which is not very significant. Madsen found that BEMT was short in accuracy when compared to the complex Navier-Stokes

CFD solution in terms of the blade root and blade tip losses [44]. But, after accounting for the Prandtl, tip, and hub loss corrections, it was concluded that BEMT may be used as an accurate performance prediction approach [37]. Therefore, BEMT remains a valuable tool for preliminary design and analysis of wind turbine blades.

In this research BEMT which is part of the QBlade software was used in the analysis of the turbines.

2.6 QBlade Software Review

QBlade is a free, relatively easy to use open-source software tool used for the development, prototyping, and simulation of airfoils or wind turbines [45]. It can be used to study horizontal, vertical axis wind turbines, and multi rotor turbines. It goes further to simulate how the turbines would operate in a wind farm enabling one to study the wake interaction effects [45], [46], [47].

The software employs various simulation methods, including: BEMT as stated earlier, the Double Multiple Stream Tube (DMST) model which was used in the study done by Altmini et. Al (2021) [46], and the Lifting Line Theory (LLT) where each element is modelled as a bound vortex and predicts lift using 3D geometry [41].

QBlade is frequently used in academic and research settings for wind turbine studies [46], [47], [48]. From the studies done by Zahariea et. Al (2019) and Koc & Gunel (2016), QBlade software demonstrated a positive agreement (within 3 percent) with Computational Fluid Dynamics (CFD) simulations [49], [50]. Therefore, QBlade software was used for the design and analysis of the wind turbines in this research.

2.7 The 5 MW NREL Reference Turbine

The NREL 5 MW turbine [51], [52] was chosen as the reference turbine for this study. The specifications of this turbine are shown in Table 2:

Table 2: 5 MW NREL Reference Turbine Specifications [52]

Rating (MW)	5
Rotor Orientation, Configuration	Upwind, 3 Blades
Control	Variable Speed, Collective Pitch
Drivetrain	High Speed, Multiple-Stage Gearbox
Rotor Diameter (m)	126
Hub Diameter (m)	3
Hub Height (m)	90
Blade Length (m)	61.5

Cut-In Wind Speed (m/s)	3
Rated Wind Speed (m/s)	11.4
Cut-Out Wind Speed (m/s)	25
Cut-In Rotor Speed (rpm)	6.9
Cut-In Rotor Speed (rad/s)	0.7
Rated Rotor Speed (rpm)	12.1
Rated Rotor Speed (rad/s)	1.3
Rated Tip Speed (m/s)	80
Overhang (m)	5
Shaft Tilt (°)	5
Precone (°)	2.5
Rotor Mass (kg)	110,000
Nacelle Mass (kg)	240,000
Tower Mass (kg)	347,460
Coordinate Location of Overall CM (m)	(-0.2, 0.0, 64.0)
Tip speed ratio (TSR) at cut-in	15.2
Tip speed ratio (TSR) at rated	7.0

This turbine was chosen because of how prominent it is used in research worldwide, and because of the extensiveness of the work that was done to develop this turbine where the authors used models from WindPACT, RECOFF, and DOWEC projects [52]. In addition, the airfoil profiles are available for free online which can then be input in QBlade for various analyses.

The airfoils incorporated in the turbine are shown in Table 3:

Table 3: Distributed Blade Aerodynamic Properties [52]

Node (-)	RNode (m)	AeroTwst (°)	DRNodes (m)	Chord (m)	Airfoil Table (-)
1	2.8667	13.308	2.7333	3.542	Cylinder1.dat
2	5.6	13.308	2.7333	3.854	Cylinder1.dat
3	8.3333	13.308	2.7333	4.167	Cylinder2.dat
4	11.75	13.308	4.1	4.557	DU40_A17.dat
5	15.85	11.48	4.1	4.652	DU35_A17.dat
6	19.95	10.162	4.1	4.458	DU35_A17.dat
7	24.05	9.011	4.1	4.249	DU30_A17.dat
8	28.15	7.795	4.1	4.007	DU25_A17.dat
9	32.25	6.544	4.1	3.748	DU25_A17.dat
10	36.35	5.361	4.1	3.502	DU21_A17.dat
11	40.45	4.188	4.1	3.256	DU21_A17.dat
12	44.55	3.125	4.1	3.01	NACA64_A17.dat
13	48.65	2.319	4.1	2.764	NACA64_A17.dat
14	52.75	1.526	4.1	2.518	NACA64_A17.dat
15	56.1667	0.863	2.7333	2.313	NACA64_A17.dat
16	58.9	0.37	2.7333	2.086	NACA64_A17.dat
17	61.6333	0.106	2.7333	1.419	NACA64_A17.dat

The first two airfoils – Cylinder1 and Cylinder2 – are circular foils. The other six airfoils were created by making corrections in the lift and drag coefficients for rotational stall delay using the Selig and Eggars method, and the Viterna method both for 0° to 90° angles of attack for an aspect ratio of 17. Then the Beddoes-Leishman dynamic-stall hysteresis parameters were estimated with no corrections to the DOWEC-supplied pitching-moment coefficients. The “DU” and “NACA” in the six airfoils refers to Delft University and the National Advisory Committee for Aeronautics respectively [51], [52].

3.0 Methodology

This section details the steps that were taken to address the objectives of this research. For the first objective, a comprehensive study was recently done by Chisale & Lee (2024) [1] and so results were synthesised from their research.

The second part will constitute the steps taken to scale down the reference NREL 5 MW turbine to the utility turbines in question: 3.5 MW, 2.5 MW, and 1.25 MW.

Finally, the stages that were done in QBlade to unravel the third objective will be explained.

3.1 Favourable Sites Considerations

The decision of where to install wind turbines depends on many factors. Although wind speed is usually the most determining factor, other factors such as slope of the area, closeness to habitats, road networks, and indeed distance to the electricity grid all play vital roles in the choice of site. It is in view of this that a comprehensive study was done by Chisale & Lee (2024) to identify the areas that would be most appropriate for the installation of wind turbines in Malawi [1]. They used GIS and AHP to identify optimal wind sites in Malawi. The integration of GIS-AHP in the spatial and land use analysis has yielded good results in countries such as Nigeria, Turkey, Sudan, Saudi Arabia, and China [53], [54], [55], [56], [57], [58].

The study used the WRF model version 4.4.1 with ERA5 reanalysis data utilized as the initial and lateral boundary conditions. A 1:3 nesting ratio was applied as is custom [1], [59] over a resolution of 4 km. Simulations on microphysics, planetary boundary layer (PBL), land surface physics and cumulus schemes were conducted over a duration of 8 days (January 15th to 23rd, 2022) similar to Shi et al. (2024) [60] who conducted their research over a 6-day period [1].

For the wind speed data, data was sourced from various wind stations in Malawi over a period between 2021-22. However, as elaborated previously, data was measured at 2 m and some of it was missing [1], [19], [61]. But for the model the wind speeds were adjusted to 10 m using the power law:

$$\frac{v_1}{v_2} = \left(\frac{h_1}{h_2}\right)^\alpha \quad \text{Equation 12}$$

where v_1 and v_2 are the wind speeds at hub height 1 h_1 and hub height 2 h_2 respectively, and α is the wind shear coefficient sometimes called the Hellman exponent with a typical value of $1/7$.

By knowing the wind speed at a certain reference hub height, one can extrapolate using the power law to get the wind speeds at different hub heights at the same geographic location.

However, α is empirically derived and varies with atmospheric stability [62], wind speed, height interval [63], and terrain roughness [64], therefore the global generalisation of $\alpha = 1/7$ was uncertain so much so that Yang et al. (2024) [65] conducted a country specific analysis of the coefficient. For Malawi it was found to be 0.206. This value was used in the research.

For the wind farm site selection criteria, six parameters were considered: proximity to settlement, road and grid, land surface slope, wind speed and the elevation which were then weighted according to the AHP: 19.3, 11.4, 11.7, 7.2, 44.3, and 6.1 percent respectively.

It was then found that six sites were suitable for wind turbine installations in Malawi. These sites were: site A at coordinates of $(-9.69635, 33.37491)$ in Chitipa, two sites in Mzimba: site B situated at coordinates of $(-11.8212, 33.74586)$ and C at coordinates of $(-11.9879, 33.57918)$, site D at coordinates of $(-13.3101, 33.8348)$ in Ntchisi, site G at coordinates of $(-14.1175, 34.18039)$ in Dedza, and site H at coordinates of $(-12.8531, 33.7712)$ in Kasungu [1].

For this study, wind patterns which were used for analysis of the 3 scaled down turbines were sourced from these areas.

3.2 Scaling Study

This section details how the scaling down of the reference 5 MW NREL turbine to the turbines of choice of 3.5 MW, 2.5 MW, and 1.25 MW was done. Several studies have been done on the effects of scaling including Burmester et al. (2016) [66] which produced encouraging results while adhering to the assumptions laid out in the books by Manwell & Rogers (2004) [67] and Gasch & Twele (2012) [68]. The assumptions include: same tip speed ratio (TSR), same number of blades, airfoils, and blade material, and making proportional adjustments to all dimensions i.e., radius, profile chord, spar size to preserve geometric similarity as much as possible.

3.2.1 Rotor Diameter

To begin the scaling process, the rotor diameter was considered since it affects the swept area by the turbine. As one would expect therefore, the smaller the turbine's power rating, the smaller the diameter. Equation 13 – adapted from the book by Professor Gasch [68] – was used to calculate the diameters of the scaled down turbines with respect to the 5 MW turbine.

$$\frac{P_2}{P_1} = \frac{R_2^2}{R_1^2} \quad \text{Equation 13}$$

where P is the power rating and R is the rotor diameter. Subscripts 2 and 1 represent the scaled down turbine and the reference 5 MW turbine respectively.

3.2.2 Rotor Speed

After the scaling down of the blade, came the rotor speed calculations. One of the assumptions under Section 3.2 is that the TSR must be kept constant in the scaled down blades. This means that the rotor speed must change in inverse proportion to the change in blade length (power and thrust are proportional to radius squared while torque to radius cubed). TSR is crucial in the design and operation of the wind turbine because, on the one hand, a very low TSR leads to most of the wind to pass through the gap between the blades reducing the effect of the lift force to aid in the rotation of the rotor. On the other hand, a too high TSR blurs the blades hindering the wind to a great extent reducing the efficiency of the turbine, and of course the greater tip speed greatly contributes to noise pollution [69]. Therefore, the following procedure was taken to make sure that the TSRs of the scaled down turbines were optimal in relation to the reference turbine.

Firstly, the TSR of the 5 MW reference turbine was calculated using Equation 14, then the equation is rearranged to Equation 15, allowing the rotation speeds for the other turbines to be calculated.

$$\lambda = \omega \frac{R}{v} \quad \text{Equation 14}$$

$$\omega = \lambda \frac{v}{R} \quad \text{Equation 15}$$

where λ is the tip speed ratio, R is the rotor radius, v is the wind speed at given hub height and ω is the rotational speed/angular velocity.

3.2.3 Chord Length

After the calculations of the rotational speed, the chord length scaling was done. Again, from the assumptions stated under Section 3.2 where it is stated that the profile chord should be proportionally adjusted to maintain geometric similarity as much as possible, Equation 16 was used to achieve this:

$$\frac{c_2}{c_1} = \frac{P_2}{P_1} \quad \text{Equation 16}$$

where c is chord length, and P is the power rating of; 2, the scaled down turbine and 1, the reference 5 MW turbine.

The chord profile for the blades of the downscaled turbines was scaled uniformly for each airfoil chord of the reference 5 MW turbine (Tab. 3).

3.2.4 Rotor Nacelle Assembly Mass

Finally, the masses of the rotor nacelle assemblies (RNA) were considered. The masses are an important factor when doing structural and financial analyses for the scaled down turbines. But due to limited time, these analyses were not conducted. Equations 17-19 from the NREL technical studies by Smith (2001) [70] and Fingersh et al. (2006) [71] and were used for the RNA components i.e., rotor blade, nacelle, hub, and tower:

$$\text{Rotor Blade Mass} = 0.1 * D^{2.63} \quad \text{Equation 17}$$

$$\text{Nacelle Mass} = 2.6 * D^{2.4} \quad \text{Equation 18}$$

$$\text{Hub Mass} = 0.24 * D^{2.58} \quad \text{Equation 19}$$

$$\text{Tower mass} = 0.3973 * A * h - 1414 \quad \text{Equation 20}$$

where D is the diameter of the rotor, A is the swept area, and h is the hub height.

3.3 QBlade

After the scaling was completed, the profiles of the scaled down were input into QBlade software for analysis. There was a problem with the circular airfoils: Cylinder 1 and Cylinder 2 where the 360 polar was not possible to simulate therefore, a new circular foil was generated. The new circular foil was along the same path as Cylinder1 and Cylinder2 airfoils from the original foils but differed in the axial turbine (at) percentage and the number of points (Fig. 8).

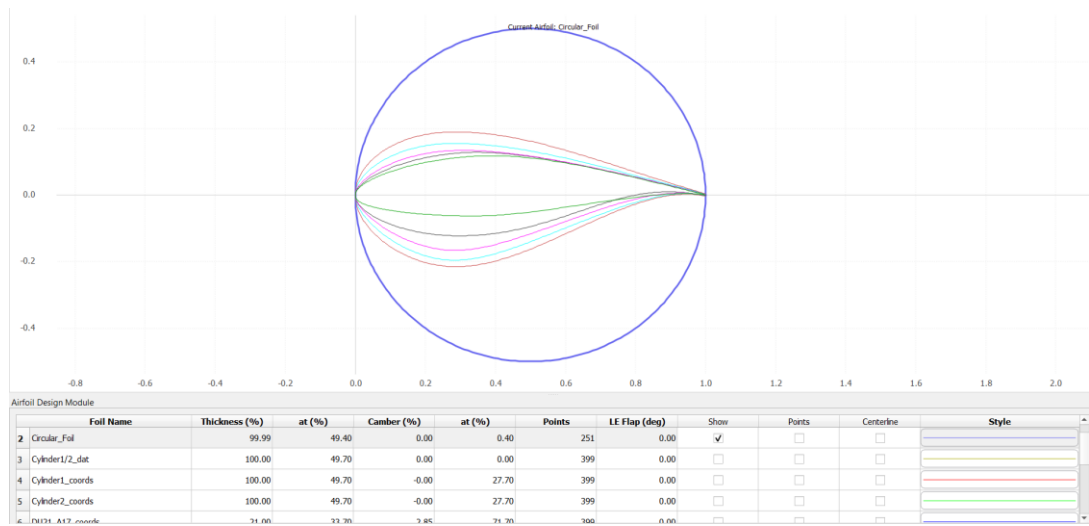


Figure 8: QBlade airfoil design module

3.3.1 Wind Speed Data

In QBlade, to get the BEMT results, wind speed data is required. Since this research was for the favourable sites Malawi, wind speed data in those sites were required. Due to the heavily disrupted wind measurement data at 2 m height by MET in Malawi [1], [19], it was better to source wind speed data from elsewhere considering also the fact that this data would need to be extrapolated to heights of 50 m, 80 m and 100 m using the power law.

ERA5 reanalysis data was considered to be the next best source. However, challenges were met to get access to this data earlier. By the time access was granted at [72], it was a little too late to re-do the analyses. Therefore, only one site was redone with ERA5 reanalysis data for comparison, and consequently this was also a sensitivity analysis for the data that was actually used for this research: global wind atlas data [73].

The challenge with global wind atlas data was that data specific to a point on the map was not possible to be obtained rather only data for the entire district that contains that geographic point could be obtained. Therefore, instead of having six areas for analysis, data for 5 areas/districts was available because the district of Mzimba had two sites that were deemed suitable in the GIS-AHP findings [1].

The downloaded data from global wind atlas was available at 100 m and 50 m. For the 80 m wind speeds, the power law (Eqn. 12) was used to calculate this taking the wind shear coefficient to be 0.206 for Malawi [1], [64], [65].

After getting the wind speeds, the frequency of occurrence for each individual wind speed value from the data from global wind atlas was calculated in Microsoft excel. Due to the large number of wind speeds, an average was calculated in intervals of 0.5 m/s to get a reasonable representation and easier to work with sample of wind speeds over the entire year.

The drawback with global wind atlas data however is that it does not provide very low wind speeds of usually not greater than 4 m/s since its purpose is more to aid policy makers to identify areas of high wind speeds that are suitable for energy production [74]. As a result, although the data is averaged over a span of 10 years, it is usually over estimated because the wind speed data, with the high values, still gives a cumulative frequency of equal to 100 percent as if the winds were that strong throughout the years.

Regardless of this limitation, for any wind turbine to be installed, wind speed data has to be recorded on site to get the real time speeds at that location. In addition, even if the low wind speeds are available, it is less likely that the change in the overall energy yield from the turbine is much due to the expected low probabilities and capacities of the low speeds from the Weibull distribution curve (Fig. 10). So, data from global wind atlas is still a good, informative source as echoed by the findings in the research by Bagder et al. (2023) [74].

The data that was used in this study from ERA5 covered a duration of 2 years similar to the study done by Chisale et al. (2024). It was sourced for the site in Mzimba with coordinates ($-11.9879, 33.57918$). This data then was processed using the same procedure described in the above paragraphs on this section for the global wind atlas data. The results were then compared against each other.

The averaged wind speeds were then used to get the corresponding power from the power curves generated in QBlade.

3.4 Power Curve

The output power of a wind turbine is commonly represented in form of a characteristic curve known as the power curve. The power curve is a relation between power output usually on the y-axis, and the wind speed usually on the x-axis (Fig. 9). It can be divided into four segments as shown on Figure 9.

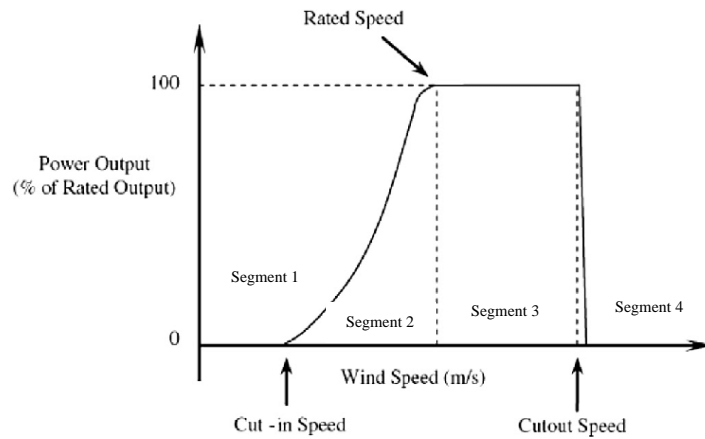


Figure 9: Generic Power Curve of a Wind Turbine

- Segment 1 is a region from wind speed 0 to cut-in speed. In this region, as can be inferred from the graph, there is no power output from the turbine because the low wind speeds are not able to generate enough torque to overcome the inertial and frictional resistive forces of the turbine [43].
- Segment 2 is a region where the turbine starts to generate some power at its cut-in speed and increases to its maximum possible power output at the rated speed.
- Segment 3 is a region between the rated speed and cut-out speed where the turbine generates the maximum power it can produce regardless of an increase in speed. This is achieved by controlling the pitch to limit the effects of the increasing wind speeds.
- Segment 4 is a region after the cut-out speed where the turbine is switched off to prevent mechanical damage to the turbine due to the excessive stress that high speeds can impose.

Power curves were generated in QBlade bearing in mind of the 4 percent loss factor associated with the ‘expected performance’ of each turbine [75], [76].

3.4.1 Annual Energy Production (AEP)

The energy yield of a wind turbine is calculated with the help of the power curve or the power formula. It is usually calculated annually because of the seasonal variability of wind. The formula used to get the annual energy production (AEP) is as follows:

$$AEP = \sum_{v=0}^{\infty} 8760 \cdot f_v \cdot P_v \quad \text{Equation 21}$$

where f_v is the frequency or the probability of occurrence of wind speed v , P_v is the power output at speed v , 8760 is the number of hours in a year, Σ is the summation from wind speed of zero to infinity.

By multiplying every frequency of a particular wind speed value with its corresponding power and multiply it with 8760 hours, we get the energy yield in megawatt hours per year.

For this study, the corresponding power of the averaged wind speed classes were deduced from the power curves in QBlade (Fig. 12). Then the values were multiplied by the corresponding frequencies of occurrence and the number of hours in a year. This resulted to the values for AEP.

Frequency of occurrence of wind speeds f_v is an important factor because from the power output equations (Eqn. 10 & 11), it can be seen that P varies with the cube of the wind speed. Therefore, the incorporation of f_v in the formula allows for a more accurate estimation of the total energy produced per year [77]. Figure 10 shows three typical curves for turbines of three classes (I, II, III) of frequency of occurrence against wind speed. The curves are the international standard for wind turbine design published by the International Electrotechnical Commission (IEC) [78], [79].

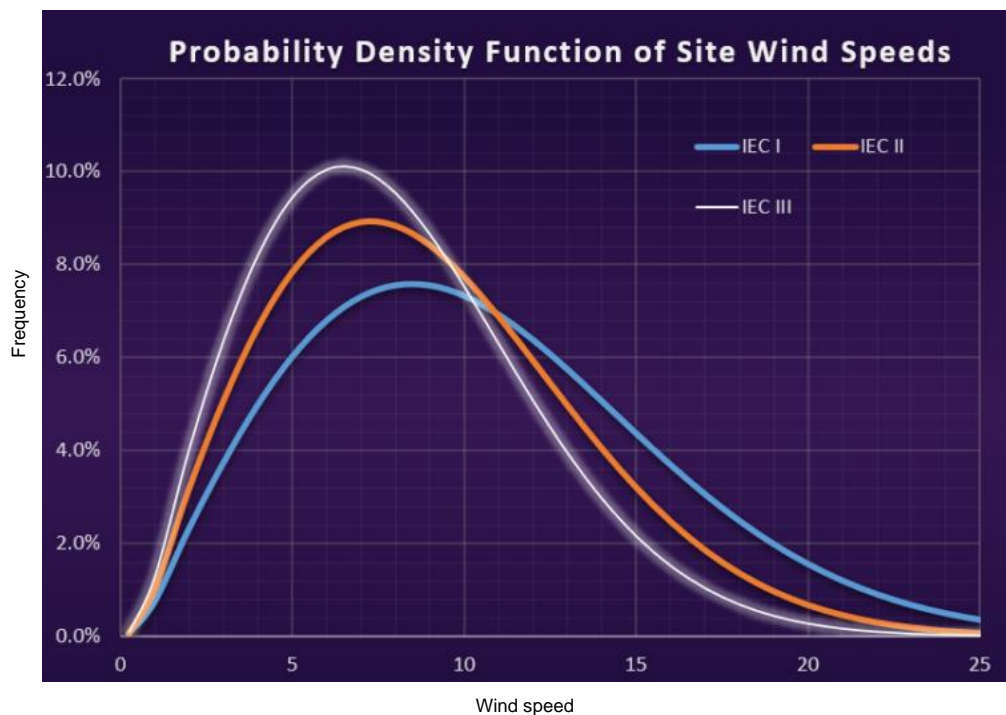


Figure 10: Wind Speed-Frequency Weibull Distribution Curve [78]

The graphs play a crucial role in the implementation of wind turbines because a wrong class of turbines should not be installed at a location where the frequency distribution is in fact for another class [78]. This is possible where the real wind speed data measured on site is different from the data used in the design process. As a result, the turbine from the design would not perform as intended that is why detailed site-specific load assessments are necessary on the design process as well.

3.4.2 Capacity Factor (C_f)

Another parameter that's used to compare the performance of wind turbines is the capacity factor C_f . It is the ratio of the amount of energy produced by a turbine over a period of time, usually one year, to the amount of energy the wind turbine would produce if it would run at its rated power throughout the duration of operation. In equation form, C_f is calculated as follows:

$$C_f = \frac{P_a}{P_r} \quad \text{Equation 22}$$

where P_a is the actual power output over the period of time, and P_r is the maximum (rated) power output over the course of the duration.

The capacity factor is not a conclusive factor in the decision of whether a turbine produces more power or not. A turbine that is producing more power annually can have a lower capacity factor than another turbine which has a lower annual energy production.

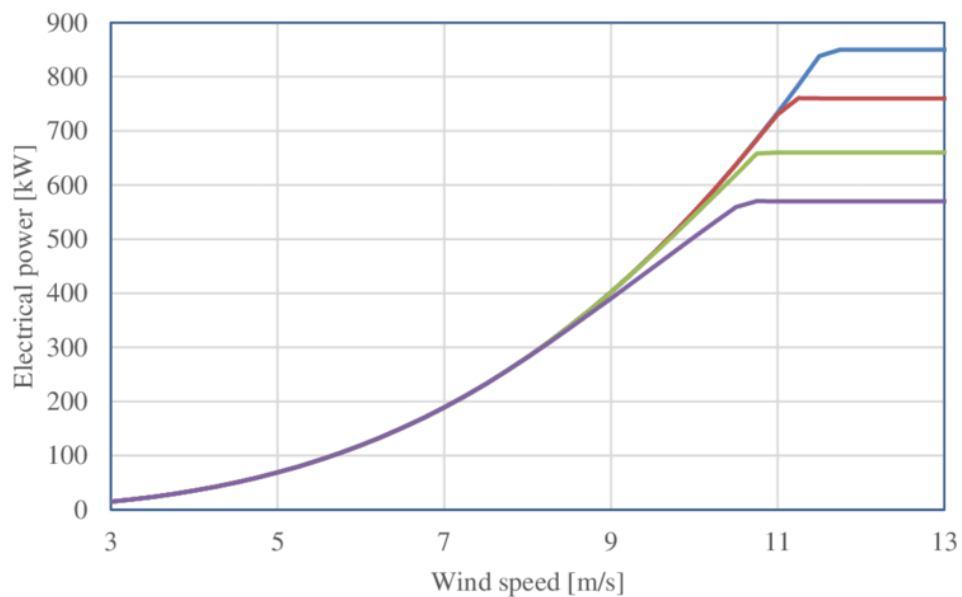


Figure 11: Power Curves for C_f Explanation [80]

Consider Figure 11 where four different power curves have been shown. Suppose the mean wind speeds in the year is 11 m/s. This would imply that the turbines responsible for the purple and green curves would have a capacity factor of 100 percent each because the turbines would operate within their rated power throughout the year. The turbines responsible for the red and blue curves would not have a capacity factor of 100 because the 11 m/s is not greater than the rated speeds of the turbines.

In terms of energy produced, the top two turbines would most likely have higher energy produced over the year than the bottom two. Nevertheless, the capacity factor is still a good indicator of the viability of a wind turbine.

4.0 Results and Discussion

This section details the results and discusses them.

4.1 Rotor Dimensions

Table 4 shows the magnitudes of the turbines after scaling down using Equation 13. The blade length was found by dividing the difference between the rotor diameter and hub diameter by 2.

Table 4: Rotor Dimensions

Rating (MW)	5	3.5	2.5	1.25
Rotor Diameter (m)	126	105	89	63
Hub Diameter (m)	3	3	2	1.5
Blade Length (m)	61.5	51.5	43.5	30.8

The dimensions are within acceptable ranges when compared to similar turbine dimensions of existing turbines. For instance, the 63 m rotor diameter of the 1.25 MW turbine compares well with the 62.3 m rotor diameter of DeWind manufacturer [81]. The blade length of 43.5 m of the 2.5 MW turbine compares well with the General Electric's (GE's, one of the world's wind turbine leading manufacturers) 2.5 MW turbine with a blade length of 44 m [82]. Finally, the rotor diameter of 105 m for the 3.5 MW turbine compares well with the aerodyn SCD 3.5/100 turbine which has a rotor diameter of 100 m [83].

However, there is a significant difference in the dimensions in Table 4 and the dimensions of the turbines that were used for analysis in Chisale & Lee (2024) [1]: Vestas 3.45 MW has a rotor diameter of 136 m [84], [85], and Gamesa 2.5 MW has a rotor diameter of 126 m [86]. This difference is a contributing factor to the difference in the power outputs that were obtained from the turbines in this study and from the study by Chisale because from Equation 11, power output from wind turbine varies with the square of the radius of the rotor blade.

4.2 Rotational Speed

Rotational speed is crucial to the design and operation of wind turbines as elaborated in Section 3.2.2. Therefore, Equations 14 and 15 were used to calculate the rotational speeds of the scaled down turbines. Table 5 shows the results.

Table 5: Rotational Speed Results

Rating (MW)	5	3.5	2.5	1.25
Cut-In Rotor Speed (rpm)	6.9	8.2	9.8	13.8
Rated Rotor Speed (rpm)	12.1	14.5	17.1	24.2

Similarly, the rotational range of 13.8 to 24.2 revolutions per minute (rpm) of the 1.25 MW turbine compares well with the maximum rotational speed of 26.1 rpm for the DeWind manufactured 1.25 MW turbine [81]. The 2.5 MW turbine’s range of 9.8 to 17.1 rpm falls within the range of GE’s 2.5 MW turbines of 5.5 to 16.5 rpm and a similar turbine SWT 2.3 MW with a rpm range of 6 to 18 rpm [82], [87]. Finally, the rated rotational speed of 14.5 rpm for the 3.5 MW turbine is equal to the rated rotational speed for the Enercon E-101 E2 3.500 [87], [88] turbine and falls within the range of the aerodyn SCD 3.5/100 turbine with a maximum rotational speed of 19.1 rpm [83].

The Gamesa G126-2.5MW turbine has a rated rotational speed of 12.5 rpm [86] which also falls within the range that most 2.5 MW turbines operate in [82], but it is lower by 36.8 percent than the rated rotational speed of the 2.5 MW turbine from this research. This difference is due to the fact that the rotor diameters – and hence the radii – were different which is a significant factor in the calculation of the rotational speed (Eqns. 14 & 15). Therefore, it further affects the power output from the turbines. The rated rotational speed of the Vestas 136-3.45 MW turbine was not provided by the manufacturer, however using similar reasoning as the 2.5 MW, it should be expected that due to the differences in the rotor blade radii, the rotational speed of the 3.5 MW turbine in this research is different from the rotor speed of the Vestas V126-3.45MW turbine.

4.3 Chord Length

The chord length was scaled using Equation 16, and the following results (Tab. 6) were obtained.

Table 6: Airfoil Chord Length

Airfoil Table	Chord Length (m)			
	5MW	3.5MW	2.5MW	1.25MW
Circular_Foil.dat	3.542	2.479	1.771	0.886
Circular_Foil.dat	3.854	2.698	1.927	0.964
Circular_Foil.dat	4.167	2.917	2.084	1.042
DU40_A17.dat	4.557	3.190	2.279	1.139
DU35_A17.dat	4.652	3.256	2.326	1.163

DU35_A17.dat	4.458	3.121	2.229	1.115
DU30_A17.dat	4.249	2.974	2.125	1.062
DU25_A17.dat	4.007	2.805	2.004	1.002
DU25_A17.dat	3.748	2.624	1.874	0.937
DU21_A17.dat	3.502	2.451	1.751	0.876
DU21_A17.dat	3.256	2.279	1.628	0.814
NACA64_A17.dat	3.010	2.107	1.505	0.753
NACA64_A17.dat	2.764	1.935	1.382	0.691
NACA64_A17.dat	2.518	1.763	1.259	0.630
NACA64_A17.dat	2.313	1.619	1.157	0.578
NACA64_A17.dat	2.086	1.460	1.043	0.522
NACA64_A17.dat	1.419	0.993	0.710	0.355

The chord lengths of the downscaled turbines were proportionally reduced with regards to geometric similarity with the 2.5 MW having a total chord length of approximately half of the 5 MW reference turbine. These were then input into QBlade for analysis.

4.4 Rotor Nacelle Assembly

The structural integrity of a wind turbine is largely dependent on the material used for the wind turbine. For scaled down turbines however the materials of the turbines are the same. Still, the structural integrity of the turbines is tested if operating at a height that’s not optimal for the turbine. Table 7 shows the masses of the RNA components – sometimes referred to as the primary elements of the wind turbine – for the scaled down turbines calculated from Equations 17-19.

Table 7: Nacelle Assembly Mass

Rating (MW)	5	3.5	2.5	1.25
Blade Mass (kg)	52,220	20,906	13,431	5,398
Nacelle Mass (kg)	240,000	186,200	124,345	54,124
Hub Mass (kg)	56,780	39,751	25,754	10,532

The tower’s mass equation (Eqn. 20) depends on hub height and the blade diameter just like the Equations 17, 18, and 19 which is good because the higher you go, the more mass you would need for the turbine to withstand the effects of greater wind speeds.

These mass values, though not exhaustive, aid in the cost analysis of the turbine system cost. After calculating these costs plus the balance of the station costs [71], the initial capital cost of a wind turbine can be found (out of scope of this project).

4.5 Energy Production

The power curves of the wind turbines generated from QBlade are shown in Figure 12.

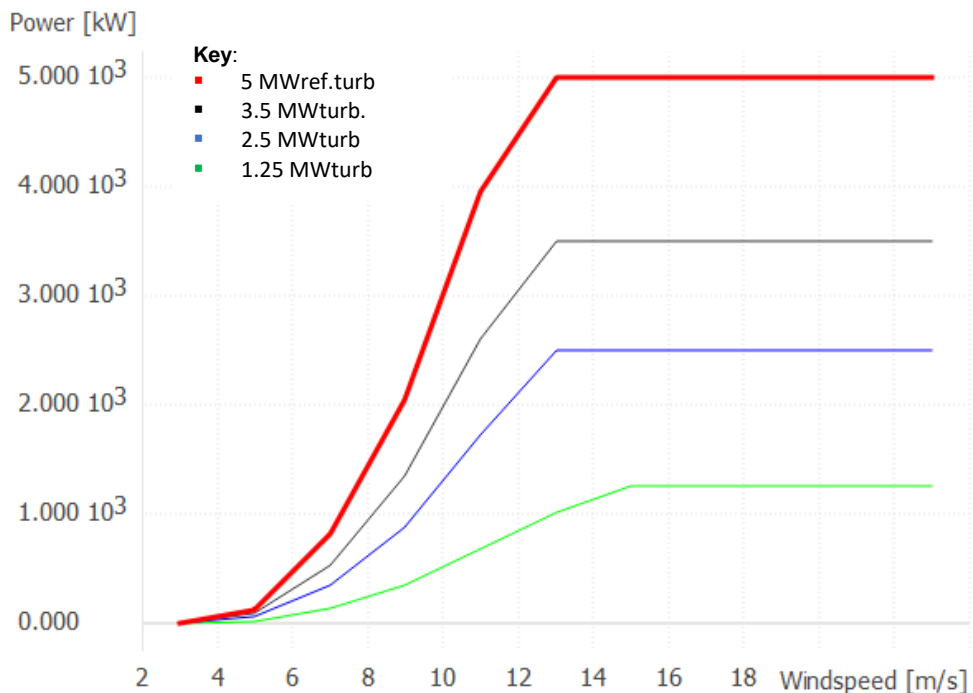


Figure 12: Power Curves of the Turbines

The rated wind speeds for the 3.5 MW and 2.5 MW turbine are the same as the 5 MW turbine because for these two, the change in Reynolds number is small enough to not affect the aerodynamic performance [41], [89], [90]. This is not the case for the 1.25 MW turbine where the rated speed has shifted to the right of the graph. This shift is due to the fact that the diameter of the 1.25 MW turbine has greatly reduced from the original so much so that it needs higher wind speeds to achieve its rated power due to the reduction in its energy capture capability. The power curves were also developed having in mind that there is a loss factor of 4 percent. These power curves were then used to calculate the energy produced per year. It is also worth pointing out that the rated speed of the 5 NREL turbine is not 11.4 m/s but it is now 13 m/s. But the fact that the rated speeds of the 3.5 and 2.5 MW turbines is the same as the 5 MW reference turbine, this change is attributed to the replacement of airfoil Cylinder1 and Cylinder2 with circular foil generated in QBlade as explained under Section 3.3.

Equation 21 was used to calculate AEP by each turbine at the favourable sites. Figure 13 shows the AEP at the different locations.

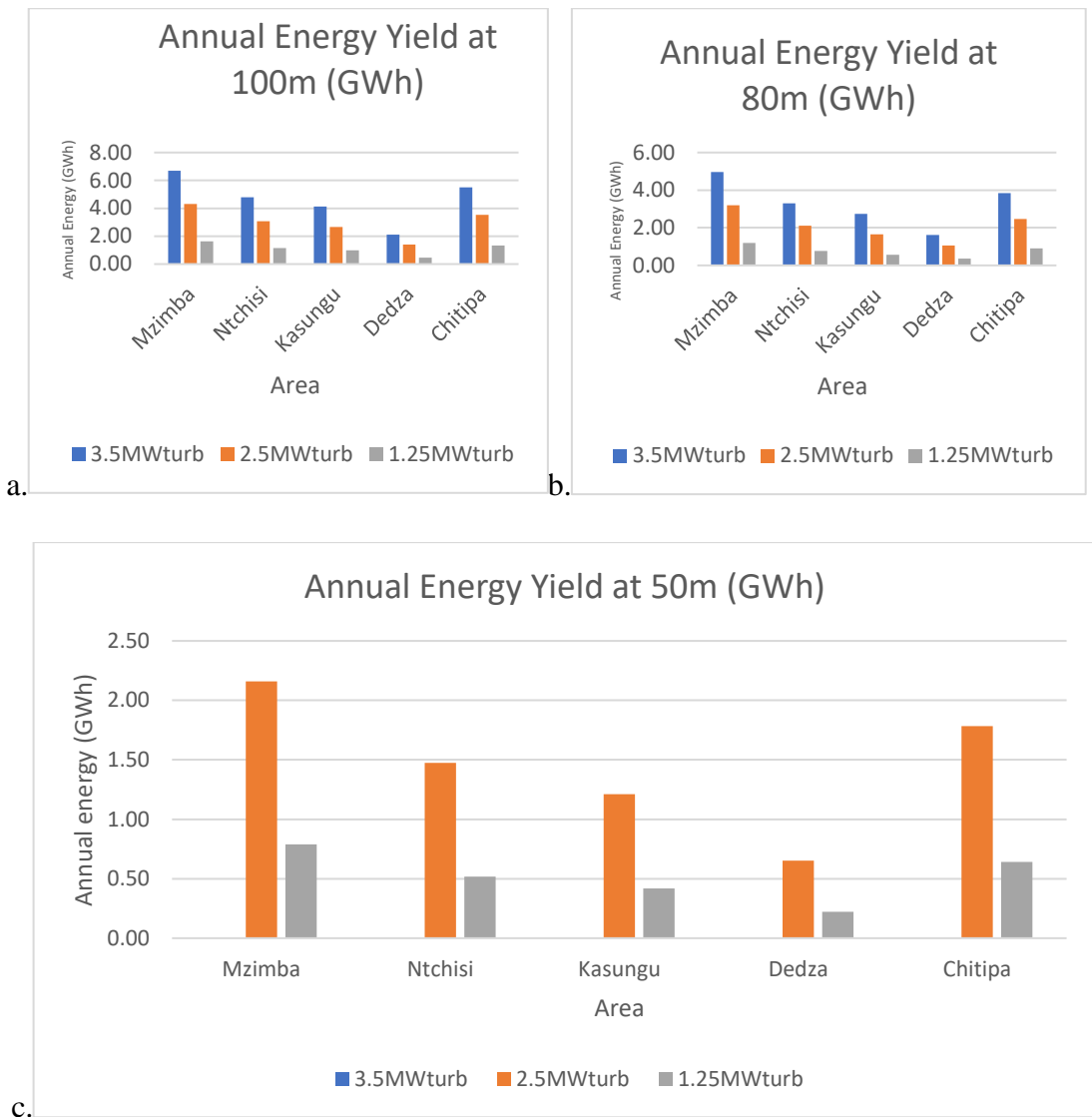


Figure 13a, b, c: Annual Energy Yield of the Turbines

It can be seen from Figure 13 that the 3.5 MW turbine produces the most energy (6.68 GWh) per year and at a height of 100 m in the district of Mzimba. This is expected because, due to its large radius and high power rating, it sweeps a large area and hence captures more wind energy. This translates to more power produced since area is an independent factor in the power equation and varies with the square of the radius.

The power produced by all turbines increases with height because wind speeds increase with altitude due to a reduction in friction with the ground and obstacles. With power proportional to the cube of the wind speed, even small changes in wind speeds greatly influence the overall power output of the turbine.

After this, the capacity factors of the turbines of the turbines were calculated (Fig. 14).



Figure 14a, b, c: Capacity Factors of the Turbines

Similarly, the site in Mzimba district has the highest capacity factors of all the other sites with the highest value of 21 percent by the 3.5 MW turbine. Of all the capacity factor values, the 3.5 MW and 2.5 MW turbines (19.7 percent) are the only ones that compare well with the standard capacity factor range of 21-52 percent for onshore wind turbines [31], [91], [92].

Sometimes it is expected that the smaller turbines can have higher capacity factors than its larger counterpart as seen in Section 3.4.2. But this is possible when all the turbines are along the same path on Segment 2 (Figs. 9 & 12) which would mean that the smaller turbine would reach its rated power quicker on the power curve. However, for this research, with each downscaling, the paths that the power curves of the resulting turbines followed were below and had a gentler slope in Segment 2 than the previous turbine (see Fig. 12) [41], [68], [93], [94]. This is the reason why the capacity

factors decreased with a decrease in the turbine size. This is another drawback in the downscaling of turbines.

The story is different however in the findings of Chisale & Lee (2024) where the capacity factors were 51.1 percent at 80 m for the Gamesa G114-2.5 turbine, and 49.94 percent at 100 m for the Vestas V126-3.45 turbine. These high values in capacity factors were attributed to the fact that the AEP was calculated using one mean wind speed value at each height of 8.72 and 8.76 m/s respectively which is a much higher over estimation than the global wind atlas data because the average speed values are regarded as if those wind speeds were available every day for 365 days, 100 percent of the time. This therefore does not give a realistic picture of the wind turbine performance at the locations. In addition, the data from ERA5 analysed for this research for a site in Mzimba at a coordinate of (- 11.9879, 33.57918) shows even much less capacity factors with highest values of 12.1 and 11.2 percent for the 3.5 and 2.5 MW turbines respectively (Fig. 15). For comparison, the same site in Chisale & Lee (2024) has capacity factors of 46.68 percent at 80 m for the Gamesa G114-2.5 turbine, and 41.91 percent at 100 m for the Vestas V136-3.45 turbine which are much higher than the average C_f value of 35 percent [31], [92].

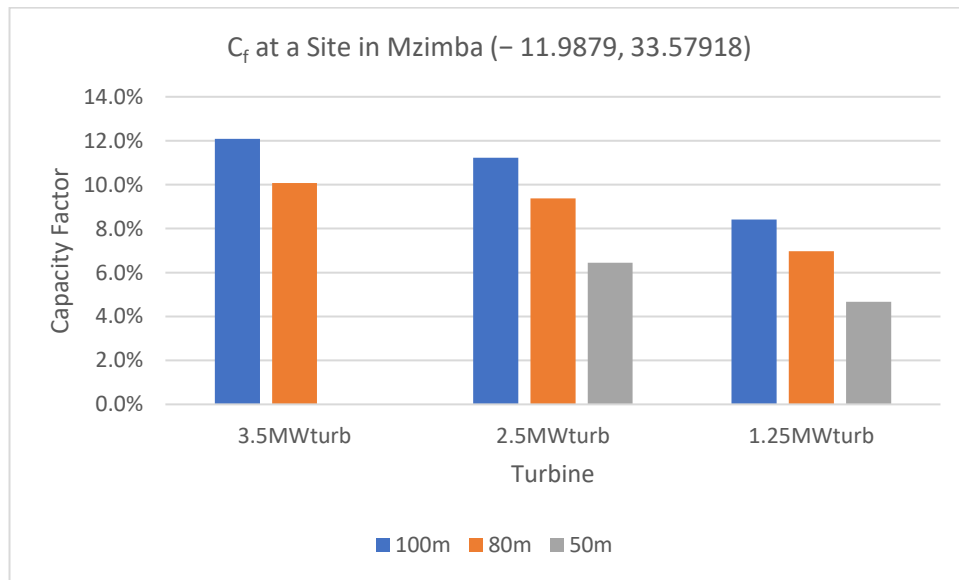


Figure 15: C_f Patterns for a Site in Mzimba

The capacity factor of the Gamesa G114-2.5 MW turbine is higher than the capacity factor of the Vestas V136-3.45 turbine because as explained above, the legs that run through Segment 2 of the power curves for both turbines are along the same path as shown in Figure 16. This means that even though the study did not do a comparative

study of both turbines at the same height, the Gamesa G114-2.5MW turbine should have a higher capacity factor than the Vestas V136-3.45 turbine at any height.

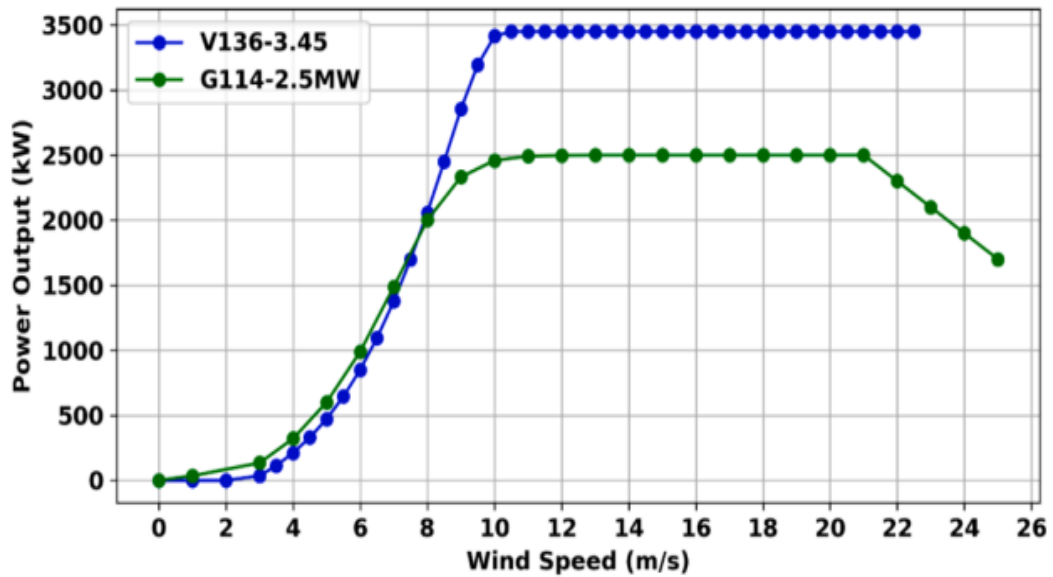


Figure 16: Power Curves of G114-2.5MW and V136-3.45 Turbines [1]

Furthermore, the AEP calculated by Chisale & Lee was for an array of wind turbines in a 50 MW wind farm scenario. This meant that wake effects were in play. With the wake effects then, it would be expected that the capacity would be low due to the wake loss rate – turbulence in the wind speeds – because no matter how much careful consideration is put into the spacing of the wind turbines on the farm, the downstream wind turbines get less of the wind [95], [96]. Of course, the differences in diameter, rated wind speed, and the power rating of the turbines, used in this research study and those in the study by Chisale et al. (2024), are critical to the discrepancies in results. Nevertheless, the capacity factors of Chisale & Lee should not be that high and so different from the results found in this study.

This is the reason why also the modelled 50 MW wind farm by Chisale et al. (2024) would serve 71701 rural buildings and 27957 urban buildings if fifteen V126-3.45 turbines were installed at the Mzimba site. For comparison, at this location, the 3.5 MW turbine would serve 719 urban buildings and 1845 rural buildings only. Even if one would neglect all the losses and wake effects and assume that fourteen 3.5 MW turbines from this study are installed on that 50 MW wind farm to give an AEP $14 * 6.68 \text{ GWh} = 93.52 \text{ GWh}$, only 25834 rural buildings, and 10071 urban buildings would be supplied for. Still falling short of the results by Chisale & Lee (2024) (The average

yearly energy demand by an urban building is 9286 kWh and for a rural building is 3620 kWh [97], [98]).

5.0 Conclusion and Further Work

In conclusion, wind energy is indeed a fast-growing industry where the technical know-how of the technology continues to expand more and more. As Malawi is on its path towards net zero, it needs to develop but by sustainable means. One way of doing this is the use of wind turbines to harness the renewable wind energy. Hence this study.

This study has presented an overview of how utility scale wind turbines of rated powers of 1.5 MW, 2.5 MW, and 3.5 MW would generally perform in five suitable districts in Malawi.

The trend that was observed in all the locations at all heights was similar in that the 3.5 MW turbine was the best performing turbine in terms of both the AEP and C_f values followed by the 2.5 MW and 1.25 MW turbine. The best location with the highest AEP and C_f values is in Mzimba indicating that this district is the most probable area for wind farm installation in Malawi. This differs from the findings of Chisale & Lee (2024) who had the best site in Chitipa. This was because although Chitipa had the highest wind speed value of all the locations, the frequency of occurrence of those high wind speeds was very low. For this research, Chitipa was second in performance to Mzimba.

The results from this study however do not give encouraging results of the performance of utility scale wind turbines in Malawi unlike in the study by Chisale & Lee. The discrepancy between the findings, as far as the energy produced per year and capacity factors are concerned, calls for further, more critical and detailed wind turbine performance assessments in Malawi.

Efforts in these further assessments for the utility scale turbines, would best be directed to the locations in Mzimba and Chitipa. The assessments would better use turbines with low specific power for the analyses like the ones used by Chisale & Lee because they have larger rotors which in turn catch more wind. These are best suited to low wind speed areas like Malawi.

Further work should include financial and detailed structural integrity assessments including the wake effects in a wind farm simulation. These assessments are important to ascertain the feasibility of the wind farm implementation. They also help in determining whether a turbine can operate better at a certain height without many

mechanical faults. It is through these analyses where one can indefinitely conclude on the optimum operational hub heights of the turbines.

Also, the turbines would need to be optimised in QBlade using either the Betz or Schmitz to maximise the aerodynamic performance of the blades.

Lastly, modelling of small to micro wind turbines (Tab. 1) with low specific power in the other suitable locations in Malawi would be a positive development. Because the results would likely lead to higher capacity factors making them economically feasible to developers due to the low overall costs associated with smaller turbines.

6.0 References

- [1] S. W. Chisale and H. S. Lee, “Comprehensive onshore wind energy assessment in Malawi based on the WRF downscaling with ERA5 reanalysis data, optimal site selection, and energy production,” *Energy Conversion and Management: X*, vol. 22, Apr. 2024, doi: 10.1016/j.ecmx.2024.100608.
- [2] IEA, “International Energy Agency,” <https://www.iea.org/regions/africa>.
- [3] CDP, “CDP AFRICA REPORT BENCHMARKING PROGRESS TOWARDS CLIMATE SAFE CITIES, STATES, AND REGIONS,” 2020.
- [4] K. Calvin *et al.*, “IPCC, 2023: Climate Change 2023: Synthesis Report. Contribution of Working Groups I, II and III to the Sixth Assessment Report of the Intergovernmental Panel on Climate Change [Core Writing Team, H. Lee and J. Romero (eds.)]. IPCC, Geneva, Switzerland,” Jul. 2023. doi: 10.59327/IPCC/AR6-9789291691647.
- [5] S. W. Chisale and H. S. Lee, “Evaluation of barriers and solutions to renewable energy acceleration in Malawi, Africa, using AHP and fuzzy TOPSIS approach,” *Energy for Sustainable Development*, vol. 76, Oct. 2023, doi: 10.1016/j.esd.2023.101272.
- [6] “REPUBLIC OF MALAWI NATIONAL CHARCOAL STRATEGY”.
- [7] World Bank Group, “Malawi Economic Monitor: Malawi’s Water and Energy Challenges can be Resolved,” <https://www.worldbank.org/en/country/malawi/publication/malawi-economic-monitor-malawis-water-and-energy-challenges-can-be-resolved>.
- [8] Government of Malawi, “MALAWI-RENEWABLE-ENERGY-STRATEGY-FINAL-VERSION-JULY-2018_2,” 2018.
- [9] E. Chaima *et al.*, “Long-term electricity demand scenarios for Malawi’s electric power system,” *Energy for Sustainable Development*, vol. 73, pp. 23–38, Apr. 2023, doi: 10.1016/j.esd.2023.01.012.
- [10] M. Kapute Mzuza and L. Sosiwa, “Assessment of Alternative Energy Sources to Charcoal in Ntcheu District, Malawi,” 2021.
- [11] Government of Malawi, “MALAWI ENERGY STATISTICS OVERVIEW,” <https://www.energy.gov.mw/statistics/>.
- [12] database.earth, “Biomass Power Plants in Malawi,” <https://database.earth/energy/power-plants/biomass-powered/malawi#:~:text=Malawi%20generates%20biomass-powered%20energy%20from%201%20biomass%20power, power%20plants%20has%20a%20capacity%20of%2010.0%20MW>.
- [13] egenco, “EGENCO,” <https://www.egenco.mw/>.
- [14] V. Soni and N. Singh, “Solar Energy Pricing,” in *Energy Systems in Electrical Engineering*, vol. Part F2133, Springer, 2021, pp. 217–229. doi: 10.1007/978-981-33-6456-1_10.
- [15] egenco, “Thermal Power Plants,” <https://www.egenco.mw/thermal-power-plants/>.

- [16] M. Mkandawire, “ESCOM spends K117 billion on Aggreko diesel generators,” <https://malawi24.com/2022/04/21/escom-spends-k117-billion-on-aggreko-diesel-generators/>.
- [17] World Wind Energy Association, “WWEA Annual Report 2023 Record Year for Windpower in 2023,” 2024. [Online]. Available: www.wwindea.org
- [18] J. D. Tan, C. C. W. Chang, M. A. S. Bhuiyan, K. N. Minhad, and K. Ali, “Advancements of wind energy conversion systems for low-wind urban environments: A review,” Nov. 01, 2022, *Elsevier Ltd.* doi: 10.1016/j.egy.2022.02.153.
- [19] C. Morton, R. Torr, R. Boddington, C. Parcell, P. Dauenhauer, and G. Ault, “Malawi Renewable Energy Acceleration Progra WEPP1-Initial Feasibility Study and Nationwide Constraints Mapping Malawi Renewable Energy Acceleration Programme (M-REAP) Initial Feasibility Study and Nationwide Constraints Mapping,” 2012.
- [20] G. W. P. Malunga, “Wind_energy_potential_in_Malawi,” 2019.
- [21] P. Tuchtenhagen *et al.*, “WRF model assessment for wind intensity and power density simulation in the southern coast of Brazil,” *Energy*, vol. 190, Jan. 2020, doi: 10.1016/j.energy.2019.116341.
- [22] C. Mattar and D. Borvarán, “Offshore wind power simulation by using WRF in the central coast of Chile,” *Renew Energy*, vol. 94, pp. 22–31, Aug. 2016, doi: 10.1016/j.renene.2016.03.005.
- [23] C. Zalengera, “A Study into the Techno-economic Feasibility of Photovoltaic and Wind Generated Electricity for Enhancement of Sustainable Livelihoods on Likoma Island in Malawi,” 2015.
- [24] egenco, “Likoma & Chizumulu Solar Power Plants,” <https://www.egenco.mw/likoma-chizumulu-solar-power-plants/>.
- [25] Ministry of Energy, “Other Renewable Energy,” <https://www.energy.gov.mw/portfolio-item/other-renewable-energy/>.
- [26] M. Lowe and G. Gereffi, “Wind Power: Generating Electricity and Employment,” 2009. [Online]. Available: <https://www.researchgate.net/publication/294579755>
- [27] Power Technology, “Power plant profile: Mzimba Wind Farm, Malawi,” <https://www.power-technology.com/data-insights/power-plant-profile-mzimba-wind-farm-malawi/>.
- [28] USTDA, “USTDA Supports Wind Power in Malawi,” <https://www.ustda.gov/ustda-supports-wind-power-in-malawi/>.
- [29] C. J. Bai and W. C. Wang, “Review of computational and experimental approaches to analysis of aerodynamic performance in horizontal-axis wind turbines (HAWTs),” Sep. 01, 2016, *Elsevier Ltd.* doi: 10.1016/j.rser.2016.05.078.
- [30] M. A. Al-Rawajfeh and M. R. Goma, “Comparison between horizontal and vertical axis wind turbine,” *International Journal of Applied Power Engineering*, vol. 12, no. 1, pp. 13–23, Mar. 2023, doi: 10.11591/ijape.v12.i1.pp13-23.

- [31] R. Wiser *et al.*, “Land-Based Wind Market Report: 2022 Edition,” 2021. [Online]. Available: <http://www.osti.gov>
- [32] B. L. Ennis *et al.*, “Optimized Carbon Fiber Composites in Wind Turbine Blade Design.” [Online]. Available: <https://classic.ntis.gov/help/order-methods/>
- [33] energy.gov, “Optimized Carbon Fiber Composites in Wind Turbine Blade Design,” <https://www.energy.gov/eere/wind/articles/optimized-carbon-fiber-composites-wind-turbine-blade-design>.
- [34] U. Lützen and S. Beji, “Predictive maintenance for offshore wind turbines through deep learning and online clustering of unsupervised subsystems: a real-world implementation,” *J Ocean Eng Mar Energy*, vol. 10, no. 3, pp. 627–640, Aug. 2024, doi: 10.1007/s40722-024-00335-z.
- [35] energy.gov, “Wind Turbines: the Bigger, the Better,” <https://www.energy.gov/eere/articles/wind-turbines-bigger-better>.
- [36] S. Khelladi, N. E. B. Triki, Z. Nakoul, and M. Z. Bessenouci, “Analysis and study of the aerodynamic turbulent flow around a blade of wind turbine,” in *Physics Procedia*, Elsevier B.V., 2014, pp. 307–316. doi: 10.1016/j.phpro.2014.07.045.
- [37] I. Masters, J. C. Chapman, M. R. Willis, and J. A. C. Orme, “A robust blade element momentum theory model for tidal stream turbines including tip and hub loss corrections,” *Journal of Marine Engineering and Technology*, vol. 10, no. 1, pp. 25–35, 2011, doi: 10.1080/20464177.2011.11020241.
- [38] P. J. Moriarty and A. C. Hansen, “AeroDyn Theory Manual,” 2005. [Online]. Available: <http://www.osti.gov/bridge>
- [39] H. Hou, W. Shi, Y. Xu, and Y. Song, “Actuator disk theory and blade element momentum theory for the force-driven turbine,” *Ocean Engineering*, vol. 285, Oct. 2023, doi: 10.1016/j.oceaneng.2023.115488.
- [40] R. Mikkelsen, F. M. Technical University of Denmark. Department of Mechanical Engineering, and MEK, *Actuator disc methods applied to wind turbines*. 2003.
- [41] R. Blanksma, E. Carmichael, F. Farmer, J. MacGregor, R. Maxwell, and S. Ordonez Sanchez, “Design Analysis of a Multi-Rotor Wind Turbine,” Frazer Farmer, 2019.
- [42] S. Gudmundsson, “The Anatomy of the Propeller,” in *General Aviation Aircraft Design*, Elsevier, 2014, pp. 581–659. doi: 10.1016/b978-0-12-397308-5.00014-3.
- [43] G. Bracco, E. Faraggiana, and D. Razzetti, “Politecnico di Torino Master degree in Mechanical engineering A Aerodynamic design of a micro wind turbine and performance analysis with QBlade.”
- [44] H. A. Madsen, R. Mikkelsen, S. Øye, C. Bak, and J. Johansen, “A Detailed investigation of the Blade Element Momentum (BEM) model based on analytical and numerical results and proposal for modifications of the BEM model,” in *Journal of Physics: Conference Series*, Institute of Physics Publishing, Jun. 2007. doi: 10.1088/1742-6596/75/1/012016.
- [45] Q, “The QBlade Software,” <https://qblade.org/>.

- [46] A. I. Altmimi, M. Alaskari, O. I. Abdullah, A. Alhamadani, and J. S. Sherza, "Design and optimization of vertical axis wind turbines using qblade," *Applied System Innovation*, vol. 4, no. 4, Dec. 2021, doi: 10.3390/asi4040074.
- [47] O. K. Zidane and Y. H. Mahmood, "Small Horizontal Wind Turbine Design and Aerodynamic Analysis Using QBlade Software," *Baghdad Science Journal*, vol. 20, no. 5, pp. 1772–1778, 2023, doi: 10.21123/bsj.2023.7418.
- [48] M. Alaskari, O. Abdullah, and M. H. Majeed, "Analysis of Wind Turbine Using QBlade Software," in *IOP Conference Series: Materials Science and Engineering*, Institute of Physics Publishing, Jun. 2019. doi: 10.1088/1757-899X/518/3/032020.
- [49] E. Koc and O. Gunel, "Comparison of Qblade and CFD Results for SmallScaled Horizontal Axis Wind Turbine Analysis," 2016.
- [50] D. Zahariea, D. E. Husaru, and C. M. Husaru, "Aerodynamic and structural analysis of a small-scale horizontal axis wind turbine using QBlade," in *IOP Conference Series: Materials Science and Engineering*, Institute of Physics Publishing, Sep. 2019. doi: 10.1088/1757-899X/595/1/012042.
- [51] old-NWTC, "5MW_baseline," https://github.com/old-NWTC/FAST/tree/master/CertTest/5MW_Baseline.
- [52] J. Jonkman, S. Butterfield, W. Musial, and G. Scott, "Definition of a 5-MW Reference Wind Turbine for Offshore System Development," 2009. [Online]. Available: <http://www.osti.gov/bridge>
- [53] T. R. Ayodele, A. S. O. Ogunjuyigbe, O. Odigie, and J. L. Munda, "A multi-criteria GIS based model for wind farm site selection using interval type-2 fuzzy analytic hierarchy process: The case study of Nigeria," *Appl Energy*, vol. 228, pp. 1853–1869, Oct. 2018, doi: 10.1016/j.apenergy.2018.07.051.
- [54] S. S. Yildiz, "Spatial multi-criteria decision making approach for wind farm site selection: A case study in Balikesir, Turkey," *Renewable and Sustainable Energy Reviews*, vol. 192, Mar. 2024, doi: 10.1016/j.rser.2023.114158.
- [55] A. S. Zalhaf *et al.*, "A high-resolution wind farms suitability mapping using gis and fuzzy ahp approach: A national-level case study in Sudan," *Sustainability (Switzerland)*, vol. 14, no. 1, Jan. 2022, doi: 10.3390/su14010358.
- [56] L. Albraheem and L. AlAwaqi, "Geospatial analysis of wind energy plant in Saudi Arabia using a GIS-AHP technique," *Energy Reports*, vol. 9, pp. 5878–5898, Dec. 2023, doi: 10.1016/j.egy.2023.05.032.
- [57] H. Eroğlu, "Multi-criteria decision analysis for wind power plant location selection based on fuzzy AHP and geographic information systems," *Environ Dev Sustain*, vol. 23, no. 12, pp. 18278–18310, Dec. 2021, doi: 10.1007/s10668-021-01438-5.
- [58] Y. Xu *et al.*, "Site selection of wind farms using GIS and multi-criteria decision making method in Wafangdian, China," *Energy*, vol. 207, Sep. 2020, doi: 10.1016/j.energy.2020.118222.
- [59] S. Tuy, H. S. Lee, and K. Chreng, "Integrated assessment of offshore wind power potential using Weather Research and Forecast (WRF) downscaling with

- Sentinel-1 satellite imagery, optimal sites, annual energy production and equivalent CO₂ reduction,” *Renewable and Sustainable Energy Reviews*, vol. 163, Jul. 2022, doi: 10.1016/j.rser.2022.112501.
- [60] R. Shi *et al.*, “Evaluation of the performance of the latest WRF model (V4.5) in simulating surface elements and its sensitivity to the diurnal SST cycle in the South China Sea,” *Clim Dyn*, vol. 62, no. 2, pp. 1567–1584, Feb. 2024, doi: 10.1007/s00382-023-06988-0.
- [61] University of Strathclyde, “MREAP STRUCTURE MALAWI RENEWABLE ENERGY ACCELERATION PROGRAMME,” 2012.
- [62] G. Gualtieri, “Atmospheric stability varying wind shear coefficients to improve wind resource extrapolation: A temporal analysis,” *Renew Energy*, vol. 87, pp. 376–390, Mar. 2016, doi: 10.1016/j.renene.2015.10.034.
- [63] H. W. Tieleman, “Strong wind observations in the atmospheric surface layer,” *Journal of Wind Engineering and Industrial Aerodynamics*, vol. 96, no. 1, pp. 41–77, Jan. 2008, doi: 10.1016/j.jweia.2007.03.003.
- [64] G. Gualtieri, “A comprehensive review on wind resource extrapolation models applied in wind energy,” Mar. 01, 2019, *Elsevier Ltd.* doi: 10.1016/j.rser.2018.12.015.
- [65] X. Yang *et al.*, “Spatiotemporal variation of power law exponent on the use of wind energy,” *Appl Energy*, vol. 356, Feb. 2024, doi: 10.1016/j.apenergy.2023.122441.
- [66] S. Burmester, S. Gueydon, and M. Make, “Determination of Scaled Wind Turbine Rotor Characteristics from Three Dimensional RANS Calculations,” in *Journal of Physics: Conference Series*, Institute of Physics Publishing, Oct. 2016. doi: 10.1088/1742-6596/753/8/082003.
- [67] J. F. Manwell, J. G. Mcgowan, and A. L. Rogers, “WIND ENERGY EXPLAINED THEORY, DESIGN AND APPLICATION SECOND EDITION ‘A very comprehensive and well-organized treatment of the current status of wind power.’” 2004. [Online]. Available: www.wiley.com/go/wind_energy
- [68] R. Gasch and J. Twele, *Wind Power Plants*, Second. Berlin: Springer, 2012.
- [69] N. Hutt, “How Fast Do Wind Turbines Spin? (20 RPM, on average),” <https://renewablesystems.org/how-fast-do-wind-turbines-spin/>.
- [70] K. Smith, “WindPACT Turbine Design Scaling Studies Technical Area 2: Turbine, Rotor, and Blade Logistics; March 27, 2000 to December 31, 2000,” 2001. [Online]. Available: <http://www.doe.gov/bridge>
- [71] L. Fingersh, M. Hand, and A. Laxson, “Wind Turbine Design Cost and Scaling Model,” 2006. [Online]. Available: <http://www.osti.gov/bridge>
- [72] IRENA, “Global Atlas for Renewable Energy,” <https://globalatlas.irena.org/workspace>.
- [73] Global Wind Atlas, “Global Wind Atlas - Malawi,” <https://globalwindatlas.info/en/area/Malawi>.

- [74] N. N. Davis *et al.*, “The Global Wind Atlas: A High-Resolution Dataset of Climatologies and Associated Web-Based Application,” *Bull Am Meteorol Soc*, vol. 104, no. 8, pp. E1507–E1525, 2023, doi: 10.1175/BAMS-D-21-0075.1.
- [75] Vestas, “Energy production Assessment Independent ingeneer,” 2021, doi: 10.5194/wes-2019-69.
- [76] T. Geer, “An Advanced Understanding of the Impact of Deviations in Turbine Performance,” 2015.
- [77] S. C. Pryor, T. J. Shepherd, and R. J. Barthelmie, “Interannual variability of wind climates and wind turbine annual energy production,” *Wind Energy Science*, vol. 3, no. 2, pp. 651–665, 2018, doi: 10.5194/wes-3-651-2018.
- [78] Wind Pioneers, “Wind Speed Frequency Distributions – Why Weibull Kills Projects,” <https://www.wind-pioneers.com/wind-speed-frequency-distributions-challenge-to-wind-farm-developers/>.
- [79] ANSI, “IEC 61400-1 Ed. 3.0 b:2007,” <https://webstore.ansi.org/standards/iec/iec61400ed2007>.
- [80] ResearchGate, “Figure 14,” https://www.researchgate.net/figure/Simulated-power-curves-for-the-Vestas-V52-for-different-maximum-tip-speeds_fig12_323319969.
- [81] The Wind Power, “D6 62/1250,” https://www.thewindpower.net/turbine_en_1210_dewind_d6-62-1250.php.
- [82] aweo, “Size specifications of common industrial wind turbines,” 2006. [Online]. Available: <http://www.aweo.org/windmodels.html>
- [83] Wind Turbine Models, “aerodyn SCD 3.5/100 nearshore,” <https://en.wind-turbine-models.com/turbines/1119-aerodyn-scd-3.5-100-nearshore>.
- [84] Vestas, “V136-3.45 MW® at a glance,” <https://www.vestas.com/en/energy-solutions/onshore-wind-turbines/4-mw-platform/V136-3-45-MW>.
- [85] Wind Turbine Models, “Vestas V136-3.45,” <https://en.wind-turbine-models.com/turbines/1282-vestas-v136-3.45>.
- [86] Wind Turbine Models, “Gamesa G126-2.5MW,” <https://en.wind-turbine-models.com/turbines/1286-gamesa-g126-2.5mw>.
- [87] © M Ragheb, “MODERN WIND GENERATORS,” 2019.
- [88] Wind Turbine Models, “Enercon E-101 E2 3.500,” <https://en.wind-turbine-models.com/turbines/1289-enercon-e-101-e2-3.500>.
- [89] A. Hasan, A. Shabur, and M. Ali, “Comparison of Aerodynamic Behaviour between NACA 0018 and NACA 0012 Airfoils at Low Reynolds Number Through CFD Analysis”, doi: 10.5281/zenodo.4003677.
- [90] S. Jha, U. Gautam, S. Narayanan, and L. A. Kumaraswami Dhas, “Effect of Reynolds Number on the Aerodynamic Performance of NACA0012 Aerofoil,” in *IOP Conference Series: Materials Science and Engineering*, Institute of Physics Publishing, Jul. 2018. doi: 10.1088/1757-899X/377/1/012129.

- [91] C. Jung and D. Schindler, “Reasons for the Recent Onshore Wind Capacity Factor Increase,” *Energies (Basel)*, vol. 16, no. 14, Jul. 2023, doi: 10.3390/en16145390.
- [92] University of Michigan, “Energy For Complete Set of Factsheets visit Wind Energy Wind Resource and Potential,” *Center for Sustainable Systems*, 2022, doi: 10.5066/F7TX3DN0.
- [93] H. Canet, P. Bortolotti, and C. L. Bottasso, “On the scaling of wind turbine rotors,” *Wind Energy Science*, vol. 6, no. 3, pp. 601–626, May 2021, doi: 10.5194/wes-6-601-2021.
- [94] K. Lin, S. Xiao, H. Liu, and A. Zhou, “Investigation on dynamic performance of wind turbines using different scaling methods in wind tunnel tests,” *Eng Struct*, vol. 284, Jun. 2023, doi: 10.1016/j.engstruct.2023.115961.
- [95] B. Sheridan, S. D. Baker, N. S. Pearre, J. Firestone, and W. Kempton, “Calculating the offshore wind power resource: Robust assessment methods applied to the U.S. Atlantic Coast,” *Renew Energy*, vol. 43, pp. 224–233, Jul. 2012, doi: 10.1016/j.renene.2011.11.029.
- [96] R. J. Barthelmie, S. T. Frandsen, M. N. Nielsen, S. C. Pryor, P. E. Rethore, and H. E. Jørgensen, “Modelling and measurements of power losses and turbulence intensity in wind turbine wakes at middelgrunden offshore wind farm,” *Wind Energy*, vol. 10, no. 6, pp. 517–528, 2007, doi: 10.1002/we.238.
- [97] A. Kalua, “Urban residential building energy consumption by end-use in Malawi,” *Buildings*, vol. 10, no. 2, Feb. 2020, doi: 10.3390/buildings10020031.
- [98] S. W. Chisale and Z. Sari, “Design of Stand-alone Solar-Wind-Hydro Based Hybrid Power System: Case of Rural Village in Malawi,” *Journal of Energy Research and Reviews*, pp. 1–16, Sep. 2019, doi: 10.9734/jenrr/2019/v3i330098.